THE STATISTICAL BOOTSTRAP MODEL

Thesis by

Christopher John Hamer

In Partial Fulfillment of the Requirements

for the Degree of

Doctor of Philosophy

California Institute of Technology

Pasadena, California

1972

Submitted: May 26, 1972

ACKNOWLEDGMENTS

I am especially grateful to Professor Steven Frautschi, my research adviser, who suggested this work at its outset, and whose constant guidance and encouragement were essential to its completion. I am also indebted to Professor George Zweig and Dr. Robert Heimann for helpful conversations and advice.

I would like to thank the Schlumberger Foundation for their financial support, and Della Harris for her expert performance at the typewriter.

ABSTRACT

A review is presented of the statistical bootstrap model of Hagedorn and Frautschi. This model is an attempt to apply the methods of statistical mechanics in high-energy physics, while treating all hadron states (stable or unstable) on an equal footing. A statistical calculation of the resonance spectrum on this basis leads to an exponentially rising level density $\rho(m) \sim cm^{-3} e^{\beta_0 m}$ at high masses.

In the present work, explicit formulae are given for the asymptotic dependence of the level density on quantum numbers, in various cases. Hamer and Frautschi's model for a realistic hadron spectrum is described.

A statistical model for hadron reactions is then put forward, analogous to the Bohr compound nucleus model in nuclear physics, which makes use of this level density. Some general features of resonance decay are predicted. The model is applied to the process of $N\bar{N}$ annihilation at rest with overall success, and explains the high final state pion multiplicity, together with the low individual branching ratios into two-body final states, which are characteristic of the process. For more general reactions, the model needs modification to take account of

correlation effects. Nevertheless it is capable of explaining the phenomenon of limited transverse momenta, and the exponential decrease in the production frequency of heavy particles with their mass, as shown by Hagedorn. Frautschi's results on "Ericson fluctuations" in hadron physics are outlined briefly. The value of β_0 required in all these applications is consistently around $[120\ \text{MeV}]^{-1}$ corresponding to a "resonance volume" whose radius is very close to $\lambda\!\!\!^{-}_{\pi}$. The construction of a "multiperipheral cluster model" for high-energy collisions is advocated.

INDEX

ACKNOWLEDGMENTS ii

ABSTRACT iii

I. INTRODUCTION 1

1.1 The Resonance Spectrum 10

1.1.1 Characteristics of the Solution 16

1.1.2 A Realistic Spectrum 22

1.1.3 Comments 26

1.2 Models of High-Energy Hadron Collisions and Other Applications 32

1.2.1 $N\bar{N}$ Annihilation at Rest 34

1.2.2 General Features of Resonance Decay 39

1.2.3 Statistical Fluctuations 46

1.2.4 High-Energy Hadronic Collisions 50

1.2.5 Other Applications 62

1.3 Summary 64

II. THE RESONANCE SPECTRUM 68

2.1 Asymptotic Form for the Level Density 68

2.2 Characteristics of the Solution 77

2.3 Quantum Numbers 81

2.3.1 Unrestricted Eigenvalues 82

2.3.2 Restricted Eigenvalues 86

2.3.3 Angular Momentum 89

2.4 A Realistic Model 94

III. APPLICATIONS 103

3.1 $N\bar{N}$ Annihilation at Rest 103

3.1.1 Pion Multiplicities 107

3.1.2 Charge Distributions 109

3.1.3 Strange Particle Production 114

3.1.4 Non-strange 2-Body Annihilation Channels 115

3.1.5 Statistical Fluctuations 121

3.1.6 Conclusions 124

IV. CONCLUSIONS 131

REFERENCES 135

I. INTRODUCTION

The literature on the statistical bootstrap model is not yet very extensive, and so in the present work we have endeavored to give a comprehensive review of the subject. Some topics are only touched on, however, which rightfully deserve a fuller discussion - such as the work of Hagedorn and his collaborators on high-energy collisions, and the several applications of the model to the field of astrophysics. For a proper discussion of these topics the reader must refer to the original papers.

The layout of the thesis is as follows. The Introduction consists of a full discussion of the subject, stating the principal assumptions of the model, their implications, and the consequences and results to be drawn from them. Its second part contains a similar discussion of the applications of the model to hadron physics, and comparisons with experiment. The detailed mathematical derivations and numerical computations, however, are relegated to Chapters II and III. So these later Chapters are essentially just appendices, to be consulted only if one requires more detail than is given in the introductory discussion. Chapter IV summarizes our conclusions.

Unless explicitly stated otherwise, numerical results throughout this work are given in units where $\hbar = m_\pi = c = 1$.

The statistical bootstrap model is basically an attempt to apply the methods of statistical mechanics to the field of high energy physics. Such methods are useful for systems in which a large number of quantum states are possible (usually because they contain large numbers of particles): for instance, a gas of particles in a box. And in elementary particle physics, one might hope that the multifarious reaction products of a high-energy hadron collision should be amenable to similar treatment. For such systems it is impossible to solve the equations of motion exactly, because of the inordinate complexity of taking care of so many degrees of freedom all at once. But in the statistical approach one makes a virtue of these many variables, and assumes that the average behavior of the system (over a long time, in the classical system; or over many events, in the quantum case) is insensitive to dynamical details. More specifically, the probability of finding the system in any particular "configuration" (specified by an overall pressure, for instance, or the average particle momentum, or any set of such observable parameters) is taken to be proportional to the density of quantum states contributing

to that configuration (i.e. to the "phase space" available). The average probability of occupation of each quantum state is assumed to depend only on overall constants of the motion for the system, such as the energy.

Such a statistical approach can only be valid if the system can be arbitrarily decomposed into sub-systems which are "statistically independent".[1] That is, the state of one subsystem must have no effect on the probabilities of different states of the other subsystems: there can be no correlations between the subsystems. This fundamental requirement is by no means always satisfied, of course; and so it is always necessary to show (or to assume!) that correlations can be neglected before statistical methods can be applied to any given system.

These methods have been used in nuclear physics with outstanding success, and a discussion thereof may be found in any standard textbook.* The applications can be divided under two main headings, namely: Bohr's "compound nucleus" theory of nuclear reactions;[2] and Bethe's statistical theory for the level density of excited nuclear states.[3] We shall give a thumbnail

---

*e.g. M. A. Preston, *Physics of the Nucleus* (Addison - Wesley, 1962), from which much of the material in the next couple of pages has been abstracted.

sketch of the assumptions involved in these two theories, and their consequences, because they are obvious prototypes for the construction of statistical theories in elementary particle physics.

The Bohr compound nucleus theory[2] grew out of the observation that low-energy neutron cross sections are generally dominated by large numbers of closely spaced, narrow resonance peaks. The reaction is therefore considered to proceed in distinct stages:

a) The incoming neutron loses its energy to the target nucleus, and is captured by it. The excitation energy is rapidly distributed among all the particles in the nucleus, resulting in the formation of a resonant "compound nucleus" state, which is a complicated superposition of single-particle and collective excitations.

b) The compound nucleus lasts for a long time, because the probability of concentrating enough energy for separation on any one particle is low, but eventually it decays. By that time it is assumed to have "lost any memory of its formation, and the only <u>correlations</u> are the very general ones associated with over-all conservation laws for the energy-momentum, angular momentum and parity of the whole system".[4]

So the reaction proceeds via long-lived intermediate states, as depicted in Figure 1. Since the compound

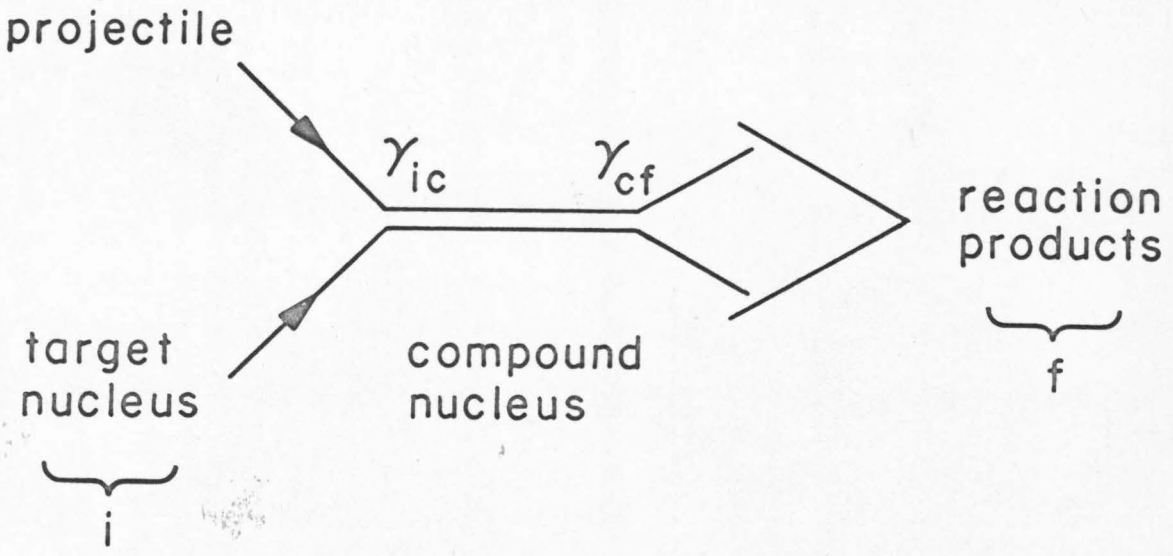

Figure 1. A compound nucleus reaction.

nucleus states "are extremely complex superpositions of different configurations, the value and sign of the vertex couplings $\gamma_{\lambda c}$ will be a random number determined by the chance values of many approximately independent other variables (the various fractional parentage coefficients in the state)".[4] This is the essential feature of the compound nucleus. Hence one can deduce:

a) Independence of formation and decay of the compound nucleus. After averaging over the resonance structure in a given energy interval, interference terms between different resonances will tend to cancel, and a reaction cross section can be written in the factorized form

$$\langle \sigma_{fi} \rangle = \langle \sigma_i(c) \rangle \frac{T}{\sum_{f'} T_{f'}} \qquad (1.1)$$

where $\langle \sigma_i(c) \rangle$ is an average compound nucleus formation cross section, and the T_f are "transmission coefficients" for the various final states f.* Thus the compound nucleus decays in the same way regardless of the manner of its formation.

---

*Strictly speaking, Eq. (1.1) is only true for each specific angular momentum and parity state. One should then sum over the allowed values of J^P.

b) Average number of neutrons emitted and their energy spectrum. An excited heavy nucleus will decay by the successive emission of one or more particles in a way very similar to evaporation from a drop of liquid.[5] The average probability of emission of a neutron of given energy, for instance, is controlled by statistical factors: it is proportional to the density of available final state reaction "channels"*, multiplied by the phase space in each channel. Hence one can predict such things as the average number of neutrons eventually emitted, and their energy spectrum (which is approximately Maxwellian, determined by a "nuclear temperature" which is in turn related to the nuclear level density).[6] Similar results can be obtained for γ-ray emission, and charged particle emission (although protons and alpha particles are inhibited by Coulomb barriers).

c) Distribution of decay widths, and level spacings. The randomness of the couplings $\gamma_{c\lambda}$ can be put on a quantitative basis:[7] this involves the theory of "statistical fluctuations". The total width

$$\Gamma_c = \sum_f \Gamma_{cf} \propto \sum_f |\gamma_{cf}|^2$$

of a compound nucleus state, for instance, is a sum of

---

*i.e. combinations of final state constituents.

squares of normally distributed quantities (the random variables γ_{cf}): it follows therefrom that the Γ_c should exhibit a χ^2-distribution, whose relative deviation from the mean goes down as one upon the square root of the number of final states available. Similarly, the resonance energies E_λ of a compound nucleus are randomly distributed: hence the distribution of the spacings between adjacent levels can be calculated[8] (it is approximately given by the so-called "Wigner distribution").

The nuclear reaction cross sections also exhibit fluctuations in energy regions where the resonances overlap and cannot be distinguished one from another. These "Ericson fluctuations" will be discussed in Section (1.2.3).

Experimental tests have confirmed the Bohr model in all these aspects a) - c), and in fact for many years it was regarded as the principal nuclear reaction mechanism.*

---

*Nowadays the importance of other mechanisms, such as "shape elastic scattering" and "direct reaction", is also recognized. In regions where those processes dominate, statistical methods are not applicable: there are strong correlations between the initial and final states.

Now at the same time that Bohr's model was being developed, Bethe[3] put forward a theory for the level density of excited nuclear states. He pictured the nucleus as consisting of two Fermi gases, one of protons and one of neutrons, confined within the usual nuclear volume (treated as a potential "box") by the nuclear forces. It can be seen that the number of nuclear states will increase rapidly as the energy is raised above the Fermi level, since the number of different ways in which one can excite combinations of nucleons out of the Fermi sea goes up sharply. The density of states of angular momentum J and excitation energy E is found to be

$$\rho^{J}(E) \simeq \text{const.} \times E^{-2}\ e^{2(aE)^{\frac{1}{2}}}(2J+1)\ e^{-J(J+1)/2cT} \qquad (1.2)$$

where a is a constant depending on the atomic number and the Fermi energies, c is a "moment of inertia", and T is the "nuclear temperature" which depends on E:

$$T \propto E^{\frac{1}{2}} \qquad (1.3)$$

After inclusion of sundry subsidiary effects (pairing forces, shell model corrections, etc.), the model is in good agreement with experiment. In particular, when combined with the compound nucleus reaction theory (paragraph b) above), it accounts very successfully for the energy spectra of neutrons evaporated from an excited nucleus.

In elementary particle physics, there arise very similar questions to those just discussed. A spectrum of resonance states occurs, and one would like to know the behavior of the level density at high energies. And it is again very important to know whether statistical methods can be applied to reactions between these particles. For convenience, we shall treat these two topics separately in what follows, although there will later turn out to be a very close connection between them - much closer than in the nuclear physics case.

1.1 The Resonance Spectrum

The statistical bootstrap approach to the high-mass hadron spectrum was pioneered by Hagedorn[9] in 1965. Important refinements were later made by Frautschi[10], however, and it is largely his point of view which we shall present in the following material.

The model is analogous to Bethe's theory of the nuclear spectrum. We consider the hadron states to be compounds of various constituents, confined within a potential box. The radius of the box will be of order one fermi, since we know that hadron structure is confined within a range of about the pion's Compton wavelength. Inside the box, the constituents are treated as non-interacting. These dynamical assumptions are very crude,

of course, but they may be improved later as our knowledge increases, just as it happened with Bethe's model.

The constituents of a hadron are assumed* to be hadrons themselves, namely all the available resonances of lower mass. This is the "bootstrap" part of the hypothesis: each hadron is a bound state of other hadrons, held together by forces which in a full dynamical theory would be due to the exchange of still further hadrons.

The resulting equation for the total density of states is:

$$\rho_{out}(m) = \sum_{n=2}^{\infty} (V/h^3)^{n-1} \frac{1}{n!} \prod_{i=1}^{n} \int dm_i \, \rho_{in}(m_i) \int d^3p_i \, \delta\left(\sum_{i=1}^{n} E_i - m\right) \delta^{3)}\left(\sum_{i=1}^{n} \vec{p}_i\right) \qquad (1.4)$$

which has the following features:

a) A factor $V/h^3 \int d^3p_i$ appears for each <u>independent</u> constituent momentum, giving the phase space available to each combination of constituents within the box of volume V. The delta functions match the total energy and momentum of the constituents to those of the compound state.

---

*These assumptions will receive further comment later on.

b) The factors $\int dm_i\ \rho_{in}(m_i)$ amount to a summation over all the possible combinations of constituents, where $\rho_{in}(m_i)$ is the density of constituent states at mass m_i. Included in $\rho_{in}(m_i)$ and $\rho_{out}(m)$ are all different states of spin, charge, strangemess and baryon number: for instance, a pion is counted as $(2I + 1) = 3$ states, and so forth.

c) The factor $1/n!$ eliminates double counting for states consisting of non-identical particles, and corresponds to Maxwell-Boltzmann statistics for states consisting of n identical particles. This counting is incorrect for configurations containing two or more identical particles in the same state (for either bosons or fermions), but the error introduced thereby turns out to be small.

The bootstrap condition has been formulated in several different ways. In a complete bootstrap theory, $\rho_{out}(m)$ would be the same as $\rho_{in}(m)$, but it is impossible to make them completely consistent in the present approximate model. In particular, at low masses one must start with some given set of input states to be used in the right-hand side of Equation (1.4), before one can generate any output states at higher mass. As a result, ρ_{in} and ρ_{out} can only be made to match properly at high mass, when the level density gets large. Three different cases have been investigated:

a) "Weak asymptotic bootstrap condition".

$$\ln[\rho_{out}(m)] \Big/ \ln[\rho_{in}(m)] \underset{m\to\infty}{\sim} 1 \qquad (1.5)$$

This was the condition originally imposed by Hagedorn[9]. It allows $\rho_{out}(m)$ to differ from $\rho_{in}(m)$ by a power of the mass. Possible solutions are*

$$\rho_{in}(m) \underset{m\to\infty}{\sim} cm^a e^{\beta_o m}, \quad a \leq -5/2. \qquad (1.6)$$

This rapidly rising exponential form turns out to be necessary in order that $\rho_{out}(m)$ should not outstrip $\rho_{in}(m)$ as the mass gets large.

b) "Strong asymptotic bootstrap condition".

$$\rho_{out}(m) \Big/ \rho_{in}(m) \underset{m\to\infty}{\sim} 1 \qquad (1.7)$$

This case was considered by Frautschi[10], and results in the small but important change that the power a must be less than, not equal to, -5/2.

---

*This form is by no means unique: for instance, Chiu and Heimann[11] have shown that a form $\rho(m) \sim cm^a e^{bm} e^{-dm^\gamma}$, $0<\gamma<1$, $d>0$, is also allowed by this condition, and by condition b).

c) "Strong bootstrap condition".

$$\rho_{in}(m) = \rho_{out}(m) + \rho_{\substack{\text{low-mass} \\ \text{input}}}(m) \tag{1.8}$$

With this formulation, first investigated by Hamer and Frautschi[12], one is making a much stronger assumption by applying a bootstrap condition at finite masses, not just asymptotically. The "low-mass input" spectrum might only extend up to some fixed cutoff mass, for instance, above which we have $\rho_{in} = \rho_{out}$. A unique solution emerges,

$$\rho_{in}(m) \underset{m\to\infty}{\sim} cm^{-3}\, e^{\beta_o m} \tag{1.9}$$

where the constants c and β_o are determined by the volume V and the low-mass input spectrum. The fact that the power a takes on the fixed value a = -3 was demonstrated numerically by Hamer and Frautschi[12], and proved analytically by Nahm[13]. Hereafter we shall consider this case only.

A numerical example[12] of such a "bootstrapped" spectrum is shown in Figure 2. A single state of unit mass was used as low-mass input, and is represented by the shaded box. Then, by a process of numerical iteration in Equation (1.4)*, a discrete spectrum satisfying Equations

*Actually, only terms with n=2 (two constituents) were kept on the right-hand side of Equation (1.4).

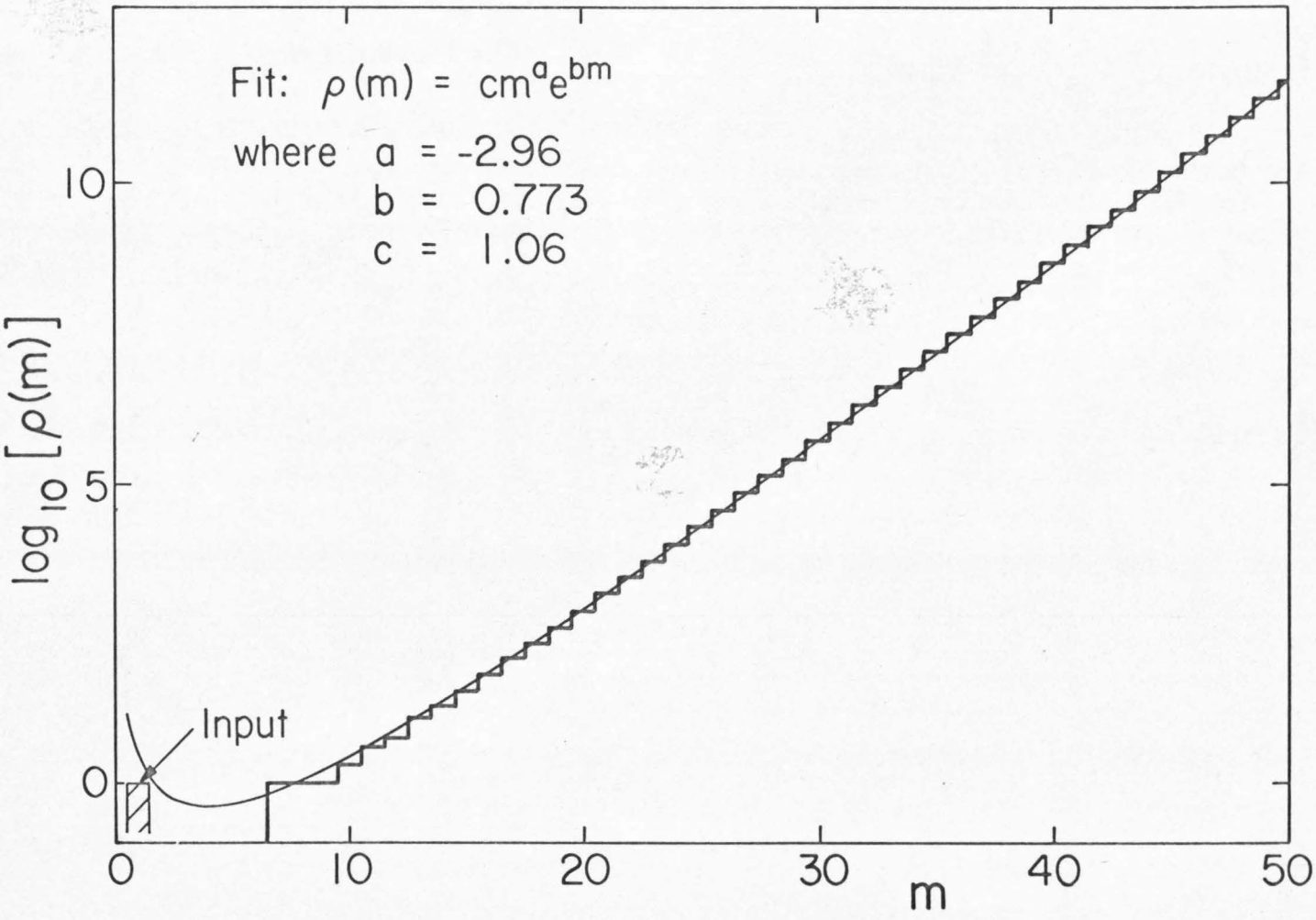

Figure 2. Bootstrap spectrum (step curve) and fit (smooth curve) in a simple case.

(1.4) and (1.8) was generated (the step curve). A least squares fit to this spectrum at large m, using the form $\rho(m) = cm^a e^{\beta_o m}$, yielded a value of a very close to -3, as shown on the figure. This asymptotic form (the smooth curve) fitted the spectrum rather well even at low masses.

1.1.1 Characteristics of the Solution

Let us now list various features of the solution which are of interest. They will be further discussed in Chapter II, and the associated mathematical proofs are presented there.

a) The parameters β_o and c. As stated above, these parameters are functions of the volume V and the low-mass input spectrum. Nahm[13] has shown that a sum rule exists for the determination of β_o:

$$H(\beta_o) = 2 \ln 2 - 1 \tag{1.10}$$

where $H(\beta)$ is the partition function for the low-mass input spectrum:

$$H(\beta) = \int dE\ e^{-\beta E}\ V/h^3 \int d^3p \int dm\ \rho_{\substack{\text{low-mass}\\ \text{input}}}(m)\ \delta(E = \sqrt{m^2+\vec{p}^2}) \tag{1.11}$$

The value of c is given by:

$$c = \left(\frac{h^2\beta_o}{2}\right)^{3/2} \frac{1}{2\pi^2 V} \sqrt{-H''(\beta_o)} \tag{1.12}$$

b) Statistically dominant couplings. An important problem is to find the most common configuration of constituents within a high-mass hadron. This was dealt with by Frautschi[10]. On substituting the asymptotic form (1.9) into the bootstrap equation (1.4), one finds that:

i) Configurations where the constituent masses add up to approximately m are favored by the exponential factors $e^{\beta_o m_i}$, so

$$\sum_{i=1}^{n} m_i \tilde{-} m \qquad (1.13)$$

Furthermore, closer consideration shows that one of these constituent masses tends to be as large as possible, while all the rest are small. The average kinetic energy of the constituents is fixed and small, of order $3/2\ \beta_o^{-1}$ (the quantity $T_o \equiv \beta_o^{-1}$ plays the role of a temperature in this model - see Section 2.2).

ii) The number of constituents tends to be small. The probability of finding n constituents in the box is given by:

$$P(n) = \frac{(\ln 2)^{n-1}}{(n-1)!} \quad , \ n = 2,3....\infty \qquad (1.14)$$

independent of mass. The average number of constituents is

$$\bar{n} = \sum_{n=2}^{\infty} nP(n) = 1 + 2 \ln 2 \tilde{-} 2.4 \qquad (1.15)$$

-69% of the time there are only two constituents in the box, 24% of it there are three, and the probability of more than three is only 7%. Equation (1.14) can be interpreted as a modified Poisson distribution in the (n-1) low mass particles: they appear almost independently of each other because each carries only a small fraction of the total energy.

iii) The probability of finding any specific heavy particle among the constituents is damped exponentially because of the statistical competition (as noted long ago by Hagedorn[14]).

All these characteristics might reasonably be expected to apply to the decay of a heavy resonance into its various possible constituents, assuming that the transition rates are dominated by statistical factors. Note in particular the prediction of small, fixed average momenta for the decay products, determined by the "limiting temperature" T_o[9]; and the predominance of decay channels with only two or three constituents. These matters will be further discussed in Section 1.2.

c) Quantum numbers. So far we have ignored the existence of quantum numbers appertaining to the various states. The equations above apply to the total density of states, and then only if no restrictions are placed on the

allowed quantum numbers of the resonances. Consider, for example, the situation when states are distinguished according to their charge Q. There are two distinct possibilities:

Case *i*): All charge states are allowed. In this case, one can employ the following argument[12] to deduce the charge distribution. A heavy resonance mostly consists of a low-mass particle with small kinetic energy (typically a pion), plus another heavy resonance which itself consists of a pion plus a resonance---etc. So the bootstrap states are mostly formed by putting pions into the box, one after another. Since these pions are equally likely to have Q=+1, 0 or -1, the probability of forming a resultant state of given charge Q becomes a random walk problem, with the number of steps (pions) being proportional to the total mass m. In the limit when m is large, the resulting charge distribution will have a Gaussian form, $\exp(-d\,Q^2/m)$, where d is a constant.

In general, if the density of states is a function of n additive internal quantum numbers $\{Q_i\}i=1..n$, for which all integer values are allowed, then the bootstrap solution is

$$\rho(\{Q_i\};m) \underset{m\to\infty}{\sim} c m^{-3-n/2}\, e^{\beta_0 m} \prod_{i=1}^{n} \sqrt{\frac{d_i}{\pi}}\, \exp\left(-d_i\, Q_i^2/m\right) \qquad (1.16)$$

while the total density of states is still

$$\rho_{tot}(m) = \sum_{\{Qi\}} \rho(\{Qi\};m) \underset{m\to\infty}{\sim} cm^{-3}\, e^{\beta_o m} \tag{1.17}$$

The constants d_i are given by:

$$d_i = \tfrac{1}{2}\,\frac{\bar{E}}{\overline{Q_i^{\,2}}} \tag{1.18}$$

where $\bar{E}$, $\overline{Q_i^{\,2}}$ are the average energy and charge squared of the low-mass input states in the box at temperature T_o: for instance,

$$\bar{E} = \int EP(E)dE$$

where the probability $P(E)$ is proportional to

$$e^{-\beta_o E} \int dm\, \rho_{\substack{\text{low-mass}\\ \text{input}}}(m) \int d^3\vec{p}\; \delta(E - \sqrt{m^2 + \vec{p}^{\,2}}) \tag{1.19}$$

Equation (1.18) has a natural interpretation: $(\overline{Q_i^{\,2}})^{\frac{1}{2}}$ is the average length of each step in the random walk, and $\bar{E}$ is the average mass interval after which each step is taken.

It is interesting that an argument of this type even works for the spin of the resonances. This more complicated problem was tackled by Chiu and Heimann[11], who showed that the bootstrap could be satisfied by:

$$\rho(m,J_z) \underset{m\to\infty}{\sim} cm^{-3}\, e^{\beta_o m} \sqrt{\frac{d}{\pi m}}\, e^{-dJ_z^{\,2}/m},\quad J_z << \frac{m}{4d} \tag{1.20}$$

where J_z is the projection of the spin in any arbitrary direction z. Then the spin J is distributed as:

$$\rho(m,J) \underset{m\to\infty}{\sim} cm^{-3}\ e^{\beta_o m} \sqrt{\frac{1}{\pi}\left(\frac{d}{m}\right)^3}\ (2J+1)e^{-d(J+\frac{1}{2})^2/m},\quad J<<\frac{m}{4d} \tag{1.21}$$

where $d = \frac{1}{2}\dfrac{\bar{E}}{\overline{J_z^2}} = \dfrac{3}{2}\dfrac{\bar{E}}{\overline{J^2}}$

the averages being taken as defined above, following Eq. (1.18).

Case *ii*): Only a restricted set of charge states allowed. This would be the situation if no "exotic" states were allowed, for instance. Then one must assume that no binding takes place in exotic channels, or that the states being generated in these channels must be thrown away. In this case it was shown by Frautschi[10] that all the partial level densities behave like the total density, and it is only the constants c that depend on the charge:

$$\rho(Q,m) \underset{m\to\infty}{\sim} c_Q m^{-3}\ e^{\beta_o m} \tag{1.22}$$

The ratios between the c_Q depend on the input spectrum. The derivation of sum rules for β_o and the c_Q in this case was considered by Nahm[13] (the earlier sum rules (1.10) and (1.12) no longer apply, because of the states which have been thrown away).

1.1.2 A Realistic Spectrum

We are now in a position to consider explicit models for the spectrum of hadron resonances in the real world. A numerical program for the construction of a model spectrum was set up by Hamer and Frautschi[12]; and asymptotic parameters for the assumed hadron spectrum have been calculated by Nahm analytically[13]. The results of the two approaches were in good agreement. Let us now outline the assumptions involved.

a) The first choice to be made is the value of the volume V. It is natural to assume that the box has a radius R of the order of one pion Compton wavelength (1.4 fermi), since this sets the maximum range of the strong interaction forces.

b) Secondly, a choice must be made of a low-mass input spectrum. Now the statistical bootstrap cannot be expected to give reasonable results until the level density becomes high; so one must simply force $\rho_{in}(m)$ to look like the experimental spectrum at low masses. Hamer and Frautschi did this by taking the lowest SU(6) multiplets* of both mesons and baryons as "low-mass input".

---

*Namely, the [35+1, L=0] mesons, and [56, L=0] baryons.

The spectrum generated by the bootstrap then looked reasonably similar to the experimental one at higher masses, up to the point where our experimental knowledge begins to break down ($\simeq$ 1.5 GeV). This is illustrated in Figure 3.

Nahm has put forward a slightly different prescription: namely, suppose that

$$\begin{cases} \rho_{in}(m) = \rho_{experiment}(m) \text{ up to (say) 1.5 GeV} \\ \rho_{in}(m) = \rho_{out}(m) \text{ at higher masses} \end{cases} \tag{1.23}$$

But the resulting spectrum is essentially the same as the previous one.

c) Finally, one must decide how to deal with the question of "exotics". In both formulations it was assumed that such states did not exist, i.e. that only meson states belonging to **1** and **8** SU(3) multiplets, and baryons belonging to **1**, **8** and **10** multiplets, are allowed.

The results obtained in the numerical model[12] will be further discussed in Chapter II. For the present we merely note that the value of β_0 turned out to be $(132 \text{ MeV})^{-1}$ for a box of radius 1.3 fermi, subject to some small numerical errors. The value of β_0 depends on the radius in a roughly linear fashion.

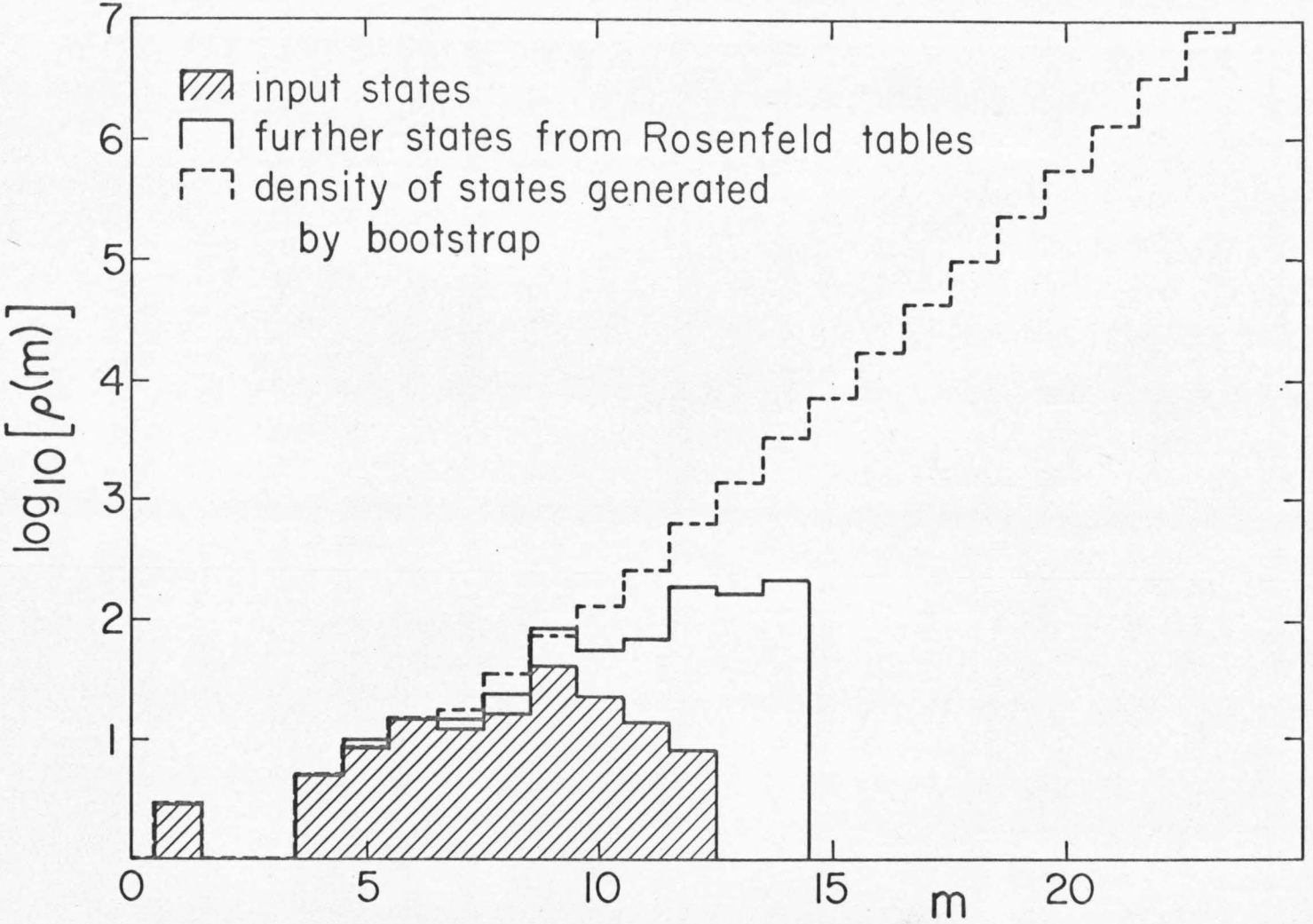

Figure 3. The bootstrap density of all hadron states compared with experiment[15] (units: $m_\pi = 1$).

The following comments may be made:

a) Figure 3 compares the total density of all hadron states as given by the bootstrap (for R = 1.3 fermi) with the density of states listed by the Particle Data Group [15]. The experimental level density rises rapidly and is roughly consistent with the theory up to energies where our detailed knowledge of the particle spectrum becomes seriously incomplete. But obviously we are very far from demonstrating by this method that the exponential rise really occurs in nature: other rapidly rising functions could fit the data equally well.

b) One of the main objects of the exercise was to see whether a specific model of this sort gave a reasonable value of the parameter β_o, similar to the value $(160\ \text{MeV})^{-1}$ obtained by Hagedorn [9] from fits to high-energy transverse momentum distributions [see Section (1.2.4)]. From this point of view, the above result is very satisfactory.*

c) Our procedure with respect to choosing a low-mass input spectrum may appear a little arbitrary, but since two reasonable alternative procedures give very similar results for the output spectrum, there is no cause for concern here.

---

*A more detailed comparison will be made in Section (3.2).

d) One may also ask whether the results are sensitive to our treatment of exotic states. If exotic states were (say) freely allowed at high energy, then the partial level densities for states of various quantum numbers would be redistributed according to the rules of Section (1.2.1); but the behavior of the total density would remain much the same. The value of β_o would increase by an amount of order 15% per each quantum number "derestricted".

1.1.3 Comments

To finish up with, we make a few rather disjointed comments on the meaning of the assumptions in the model, and its overall validity.

a) Connection with duality. Dual models of the scattering amplitude, such as the Veneziano scheme[16], give very similar results to those of the statistical bootstrap for the level density. The reason is not hard to find[17,10]. Duality implies that the scattering amplitudes in every channel are dominated by narrow resonances, which add up at high energy to give the overall Regge behavior. Factorization then implies that at each energy where a counting is performed, the number of resonances must be at least equal to the number of scattering channels open. This bears a close resemblance to the statistical bootstrap assumption that resonances are formed in every channel at

a rate proportional to the phase space available to the constituents, within a box of volume V. In both cases, that is, the rate of increase of the number of resonances at a given energy (and thus of the number of scattering channels, as it turns out) is proportional to the number of channels already open; this necessarily produces an exponentially rising level density. In the Veneziano case, the result is actually

$$\rho(m) \sim c m^{-5/2} {}^{-n/2} e^{\beta_n m} \qquad (1.24)$$

where n is the number of "extra dimensions" of the oscillator operator in that model[16,18]. Even the values predicted for the parameter β are similar in the two models. But the details of their structure are quite different, particularly as concerns the distribution in angular momentum [see Section (2.3)].

b) Accounting for strong interactions. Our treatment of exotic states highlights the question: what exactly are we assuming about the strong interactions among the hadrons? By throwing away all exotics, we assume that the forces are always non-attractive in these channels. But maybe the true situation is that a spectrum of such states does exist, and is merely delayed to higher masses than have been explored experimentally at the present time. This state of affairs might be simulated by raising the 'floor' of our potential box by some average energy, in order to represent an initial repulsion in these channels.

But are we treating the attractive forces correctly? The walls of the box should correctly account for the phase space effects due to the finite range of the strong interactions.* But what about the strong interactions between particles within the box? Won't they have a drastic effect on the density of states?

The answer is that we have already assumed consistently attractive forces between all combinations of hadrons (except exotic ones) by counting the bootstrapped resonant states as independent particles. Consider, for example, two particles in a box with their relative wave function having an lth partial wave

$$\Psi_l(r,p) \sim {}^1/_r \sin\,(pr - {}^{l\pi}/_2 + \delta_l) \tag{1.25}$$

The boundary condition at the wall of the box (r = R) gives

$$pR - {}^{l\pi}/_2 + \delta_l = \pi n_l \ , \ n_l = 0,\ 1,\ 2... \tag{1.26}$$

so we have

$$\pi \frac{dn_l}{dp} = R + \frac{d\delta_l}{dp} \tag{1.27}$$

---

*One might ask what happens if the volume of the box changes with the mass of the resonance. This has been explored by M. Alexanian (*Phys. Rev. D4*, 2432 [1971]). The asymptotic form of the mass spectrum changes radically as one might expect. But it is hard to find a physical reason why such a thing should happen.

Thus, an attractive force gives $d\delta_l/dp > 0$ and increases the density of states in the box, a repulsion gives $d\delta_l/dp < 0$ and decreases the density of states. At the position of a narrow resonance of angular momentum l, the phase shift δ_l suddenly increases by π, allowing one extra state into the box. So if the phase shift is dominated by a narrow resonance, one can count the number of states in the box by treating the original particles as non-interacting, but including states of motion of the resonance as well.

So the statistical bootstrap assumptions can be viewed in another light as follows:

i) Attractions exist between all (non-exotic) sets of particles sufficient to bind them within a volume V;

ii) The relative phase shifts (i.e. scattering amplitudes) are dominated by narrow resonances, which can then be treated as stable, independent particles participating in new reaction channels.

This idea of including attractive forces by counting resonant states was originally due to Beth and Uhlenbeck[19], and was first applied to hadron physics by Belenky[20]. Essentially the same thing is done in classical thermodynamics[21]: if one wishes to describe a gas of hydrogen molecules, one doesn't deal with the component atoms plus all the forces responsible for binding them together.

Instead, he deals with configurations of the bound states, the molecules themselves, and ignores all interactions entirely.

Note that the maximum effect repulsions in any channel can have is to prevent formation of resonances in that channel. In Equation (1.27), for example, the quantity $\frac{d\delta_l}{dp}$ is restricted by Wigner's bound[22]:

$$\frac{d\delta_l}{dp} \geq - R \qquad (1.28)$$

As long as there is a class of scattering channels in which attractions consistently occur, the bootstrap solution will hold and the spectrum rises exponentially.

The bootstrap idea is also compatible with a suggestion by Mandelstam[23], that it is the opening of new scattering channels, in which new resonances may be formed, which accounts for the linear rise of the hadron Regge trajectories. Such behavior is in marked contrast with the result of non-relativistic potential models, where one expects the trajectories to turn over and reach an "ionization point": the only other alternative is to invoke

an infinite potential well, as in the harmonic oscillator quark model, which is probably unphysical.*

It has been remarked by van Hove[24] and Durand[25] that one can combine the narrow-resonance approximation with Regge asymptotic behavior if and only if the trajectories rise indefinitely. Thus a turnover point for the trajectories would mark the limit at which the narrow resonance approximation becomes invalid, and both the statistical bootstrap and dual resonance models break down.

c) Experimental tests of the model. Unfortunately, the asymptotic form of the level density of hadrons cannot be determined directly. In the nuclear physics case, the compound nucleus states are very long-lived, and show up nicely as narrow peaks in the cross-section: thus Bethe's formula (1.2) could be verified simply by counting the

---

*Of course, we have also used an infinite well, i.e. our potential "box". But this is not important to our result: binding may cease to occur in any one channel after the first several resonant states have been formed, but by then the newly opened "inelastic" channels will have taken over, and will keep the level density rising exponentially.

number of states per unit energy.* In the elementary particle case, on the other hand, the states are hundreds of MeV wide, so as soon as they become densely distributed it becomes impossible to sort out one from the other. As stated in the previous Section, the model is roughly consistent with the experimental spectrum, but that is the most one can say.

Therefore one must turn to more indirect methods in order to test the theory. For instance, it has been incorporated by Hagedorn[9] and others in a model of high-energy hadron reactions. Insofar as experiment agrees or disagrees with the important predictions of this model for reactions, the assumptions involved in the model for the spectrum will also be supported or denied. In the next Section it will be shown that the outlook here is encouraging.

1.2 Models of High-Energy Hadron Collisions, and Other Applications

The high-energy reactions of hadrons, in which quite large numbers of secondary particles are usually produced, seem at first sight to offer a good opportunity to use the

*Actually, a direct count of the resonance levels is only possible over a narrow range of energies in this case also, and does not provide an entirely conclusive test of the model.

statistical approach. It was very early proposed by Fermi[26] that the energy released would rapidly distribute itself according to statistical laws among the various degrees of freedom available within a hadronic "interaction volume" V', of order $\frac{4\pi}{3}\left(\frac{\hbar}{m_\pi c}\right)^3 \equiv \Omega_o$ in size. Then the relative probability of decay into each final state can be predicted: it is simply proportional to the phase space available to that state within V'.

It soon became apparent, however, that this idea was incorrect in its simplest form. There are found to be important correlations between the incoming particles and the outgoing ones, as demonstrated by the strong tendency of the reaction product momenta to be aligned in the forward or backward directions. Thus the fundamental assumptions of the statistical approach are violated.

Recovering from this setback, various groups have gone on to modify the approach, attempting to take account of the correlations and then treat the remainder of the problem statistically. We shall return to this subject in Section (1.2.4).

There remains one reaction where it may be that no modification is necessary, namely nucleon-antinucleon annihilation at rest[27]. In this case the incoming momenta are zero, so that gross correlations of the above sort cannot occur. The energy released is quite high, and so is the multiplicity of reaction products, so that

statistical considerations should be applicable. Furthermore, the experimental data are abundant[28]. We shall now discuss a statistical bootstrap approach to this problem[29].

1.2.1 $N\bar{N}$ Annihilation at Rest in the Statistical Bootstrap Model

The object of the statistical model is to reproduce the multiplicity distributions, momentum spectra and angular correlations of the annihilation products (mainly pions). There is only one parameter available within the simplest version of the model, namely the volume V'. Even failures of the model may be useful: they can isolate important dynamical effects which have not been taken into consideration, in analogy to the way that resonances appear as bumps superimposed on the "statistical" phase space curves when mass spectra are plotted for a single reaction channel.

Originally, only states consisting of non-interacting pions (and kaons) were taken to comprise Fermi's "degrees of freedom" mentioned above. But then the interaction volume required to match the experimental pion multiplicity turns out to be of order $6\Omega_o$, which is too large to be plausible physically. It was soon recognized[2] that this was due to strong attractions between the pions, which

allow more of them to be squeezed into a given volume than the non-interacting model predicts. It was then that Belenky[20] showed how within the narrow resonance approximation the two-body attractions could be taken care of by counting resonant states, as well as stable particles such as pions, among the possible constituents within the interaction volume [see Section (1.1.3)].

Various authors attempted to implement this idea using a restricted list of resonances such as the ρ[30], or all the pseudoscalar and vector mesons[31]. A good deal of improvement was obtained, but they still found it necessary to use either a large volume, or unphysically low resonance masses, in order to reach agreement with experiment. But now, with the advent of the statistical bootstrap model of Hagedorn[9] and Frautschi[10], it has become possible to carry Belenky's idea to its logical conclusion. The statistical bootstrap provides a model for the spectrum of resonances above those which are presently known, so one can now include all resonances with mass less than the energy released by the annihilation process. Our picture of the decay process then becomes a "democratic" one, in which it is assumed that the $N\bar{N}$ system decays into any given combination of hadrons at a rate proportional to the phase space available to those hadrons within the $N\bar{N}$ interaction volume V', and no distinction is made between

"stable" particles such as the π and K mesons, and the unstable resonant states.

If one pictures $N\bar{N}$ annihilation at rest as taking place via resonant intermediate states, just as in Bohr's compound nucleus model of nuclear interactions, then our statistical model of the decay process, and the Hagedorn-Frautschi model for generating the hadron spectrum, are seen to be but two sides of the same coin. The density of resonant states at a given mass is just equal to the density of "scattering states" into which the resonances may decay. In particular, the $N\bar{N}$ "interaction volume" V' and the "resonance volume" V of Equation (1.4) are expected to be one and the same. The annihilation process will proceed via the mechanism shown in Figure 4, with the final state pions (or kaons) being produced at various stages of a long decay chain.

In comparing this model with experiment*, the radius R was taken to be an adjustable parameter. But one expects R to lie somewhere near one pion Compton wavelength; otherwise the validity of the model would be very dubious. In the event, the radius required to match the experimental pion multiplicity turned out to be $(1.14 \pm 0.18)\lambda\!\!\!^{-}_{\pi}$, or 1.6 ± 0.25 fermi, a not unreasonalbe figure. The corresponding value of β_o is $(107 \pm 20 \text{ MeV})^{-1}$.

*Details will be found in Chapter III.

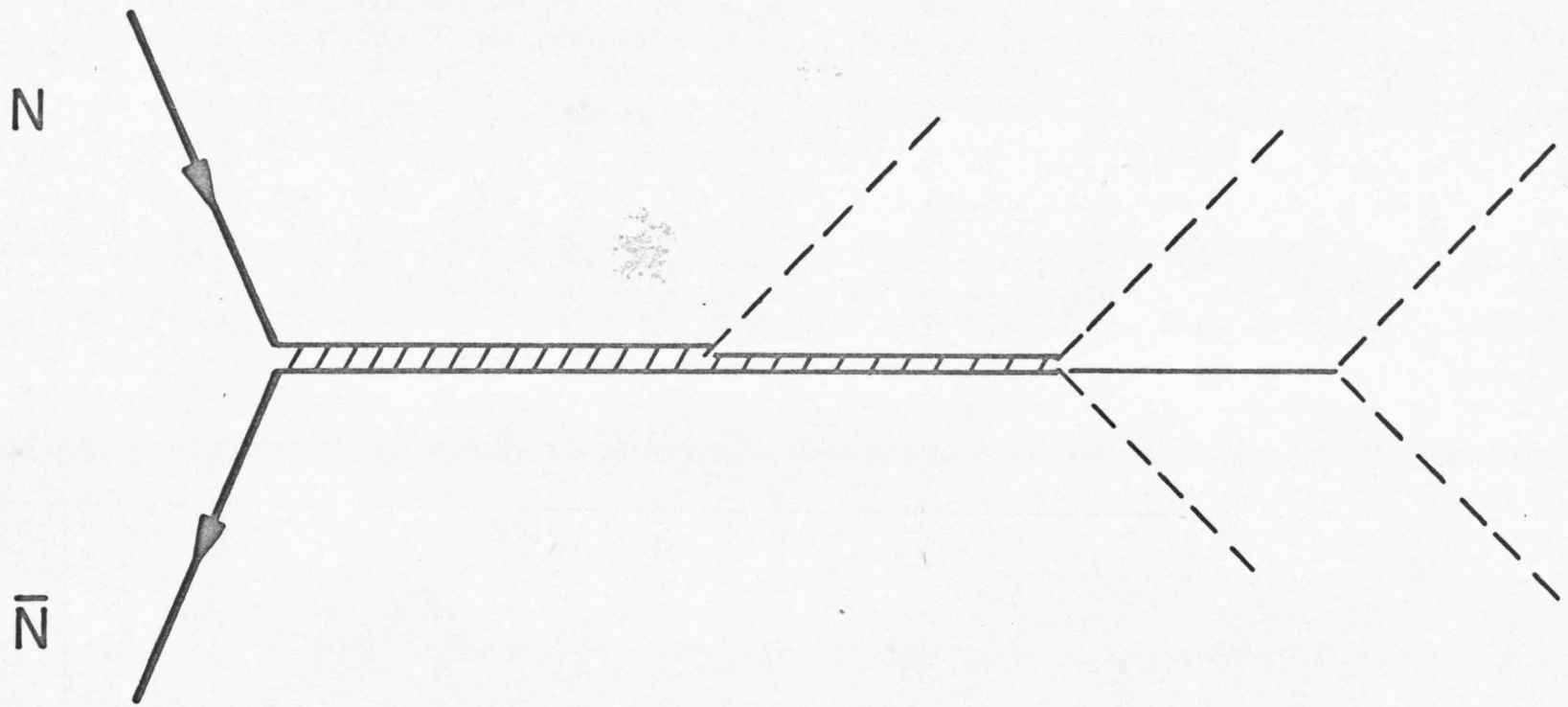

Figure 4. $N\bar{N}$ annihilation process and subsequent decay chain.

Comparison with data showed that:

a) The overall pion multiplicity, and the charged prong frequencies, are well fitted.

b) The branching ratios into specific multi-pion charge states are fitted satisfactorily, except for two or three channels which are theoretically expected to be heavily populated, but where the experimental figures turn out too low. Neutral pions seem to be more numerous than expected.

c) The model predicts too many annihilations into final states containing $K\bar{K}$ pairs. The suppression of these channels seems largely to be due to Zweig's famous rule[32], which forbids processes involving disconnected quark graphs: for instance, the production of Ø-mesons in the present case. The pion multiplicities associated with strange events are fitted quite well.

d) The branching ratios into specific non-strange two-body resonance channels are fitted, on the <u>average</u>, about as well as could be expected.

The statistical bootstrap picture thus explains two important features of the experiments which had previously been hard to understand. The first is the high multiplicity of final state pions ($\langle n_\pi \rangle = 4.7 \pm 0.1$), which we can now attribute to the effect of strong attractions allowing more pions to be crowded into the box. The second is the small size of the individual two-body branching ratios

(typically of order 1%), which is due to the large number of competing channels which are open. These successes therefore provide experimental evidence for the underlying assumptions of the statistical bootstrap.

The failure of the model with regard to strange particle production is somewhat less significant. It demonstrates the existence of an unconsidered dynamical mechanism which suppresses such events: a phenomenon which has actually been known for quite some time[33]. The overabundance of neutral pions is so far unexplained; it might conceivably be due to Bose statistics.

1.2.2 General Features of Resonance Decay

The model outlined in the previous Section can immediately be generalized to describe the decay of any high-mass resonance, via a chain of events as in Figure 4. Such a model might be applied, for instance, to the decay of a "fireball"[9] produced in a high-energy collision, ending up as a cluster of final-state particles with low relative momenta.

Since the decay branching ratios are assumed to be governed by phase space, the characteristics of Section (1.1.1 b)) apply <u>at each vertex</u> of the decay chain:

a) The probability of decay into n constituents is given by

$$P(n) = (\ell n 2)^{n-1}/(n-1)! \qquad (1.29)$$

so that two- and three-body decays predominate.

b) Of these constituents one tends to be heavy, and the remainder light. The kinetic energy released is small.

c) The probability of finding a specific heavy particle among the constituents goes down exponentially with its mass.

Let us now concentrate on the π-mesons emitted during the whole decay process. Those emitted at each separate vertex have a fixed average kinetic energy of order $(3/2)T_o$, and the recoil of the heavy secondary resonances can be neglected until the very end of the decay chain. Therefore the average number of pions emitted should be simply proportional to the mass of the initial resonance: this was first remarked by Hagedorn[34]. The results of a numerical calculation are shown in Figure 5, the radius R having been adjusted fo fit $N\bar{N}$ annihilation at rest (see previous Section). It can be seen that a linear relationship between $\langle n_\pi \rangle$ and the mass of the resonance is established immediately, with

$$\langle n_\pi \rangle = 0.6 + 0.30\ (m/m_\pi) \qquad (1.30)$$

It would be interesting to see whether the multiplicity $\langle n_\pi \rangle$ does in fact rise in this fashion for $p\bar{p}$ annihilation in <u>flight</u> over the first several hundred MeV/c above

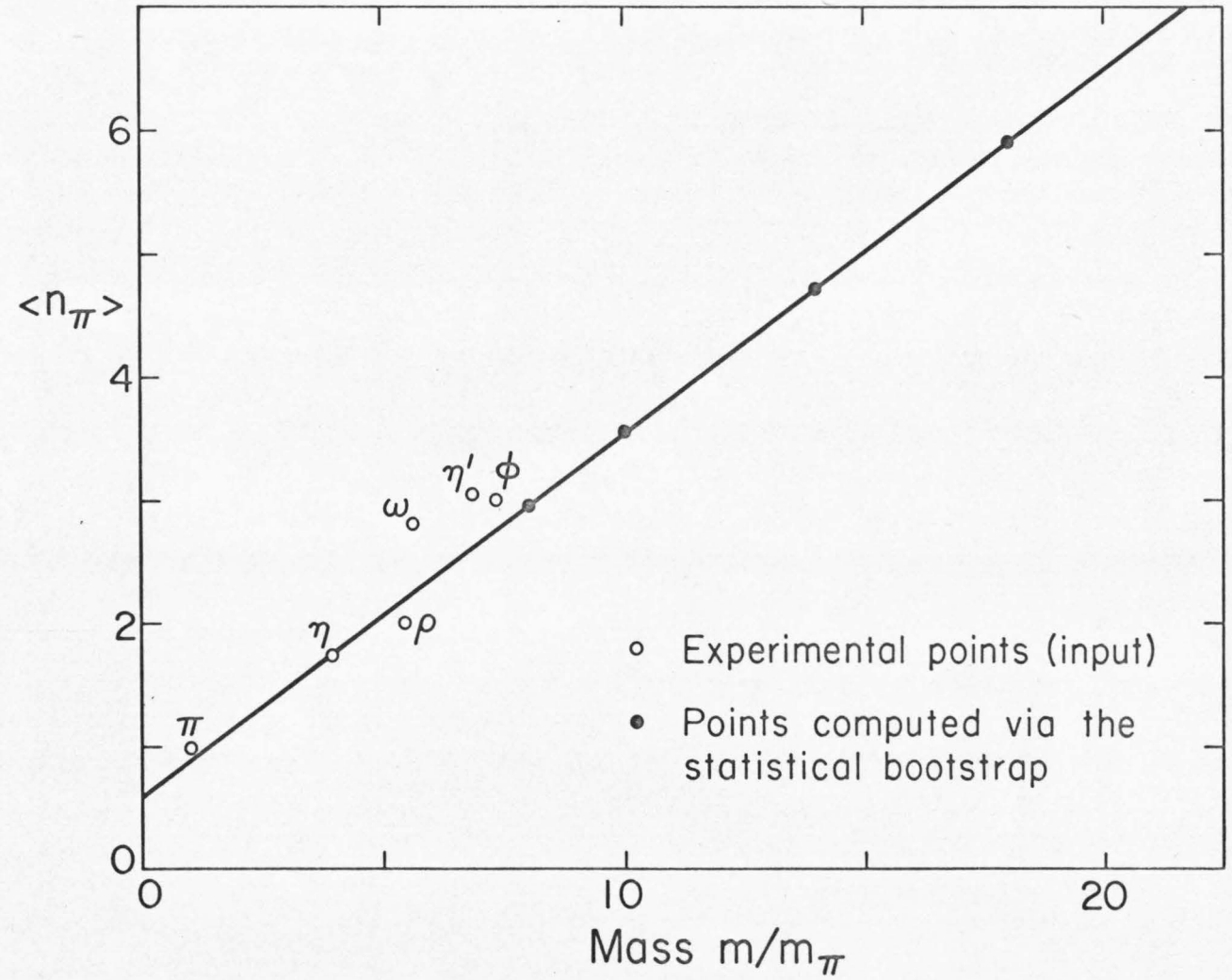

Figure 5. Average number of pions in the final state after non-strange decay of resonances of strangeness zero. Experimental points are from the Particle Data Group tables[15]. Box radius R = 1.6F.

threshold, a region where the main assumptions of the present model should still hold reasonably well. Unfortunately no experimental data seem to be presently available in this range. We cannot test the prediction directly on states listed in the Particle Data Group tables[15] either, because the model will not apply to resonances of low mass or high angular momentum, i.e. those lying on the leading Regge trajectories.

The momentum distribution of the emitted pions should be essentially of the Maxwell type:

$$P(p_\pi) \propto p_\pi^2 \exp\left[-\sqrt{m_\pi^2 + p_\pi^2}\,/\,T_{eff}\right] , \qquad (1.31)$$

where $P(p_\pi)$ is the probability of finding a pion in the final state with a momentum of magnitude p_π, and T_{eff} is an "effective temperature" such that $T_{eff} \gtrsim T_o$. The distribution cuts off exponentially at large momenta because the resonance spectrum cuts off exponentially at low mass, in this model. There are important modifications to the form (1.31), however, at both the low momentum and high momentum ends of the distribution. For details, we refer to Section (3.2).

The multiplicity distribution of the emitted pions can be found by the following argument. The kinetic energy distribution of the pions emitted at any single vertex has a Maxwell-Boltzmann form like (1.31) above;

but when one averages over all the pions emitted in a long decay chain, then by the central limit theorem the distribution in average kinetic energy $\langle T_\pi \rangle$ will be a Gaussian. Therefore, since

$$\langle n_\pi \rangle = \frac{m}{m_\pi + \langle T_\pi \rangle} \tag{1.32}$$

the multiplicity distribution will also be a Gaussian (presuming it to be fairly narrow). The numerical results for $\bar{p}p$ annihilation at rest illustrate this behavior (Figure 6). The standard deviation of this multiplicity distribution should vary like the square root of $\langle n_\pi \rangle$, i.e. like the square root of the mass, and once again this is borne out by the numerical calculations. The standard deviation quickly settles down to a form

$$\sigma_{n_\pi} = 0.26 \sqrt{\frac{m}{m_\pi}} \tag{1.33}$$

We note that the multiplicity distribution comes out much the same whatever the SU(3) quantum numbers of the initial state (provided of course that it has strangeness zero).

The distributions of other particles emitted in the decay of a heavy resonance (such as ρ mesons, $K\bar{K}$ pairs, and $N\bar{N}$ pairs) should follow laws similar to the above.

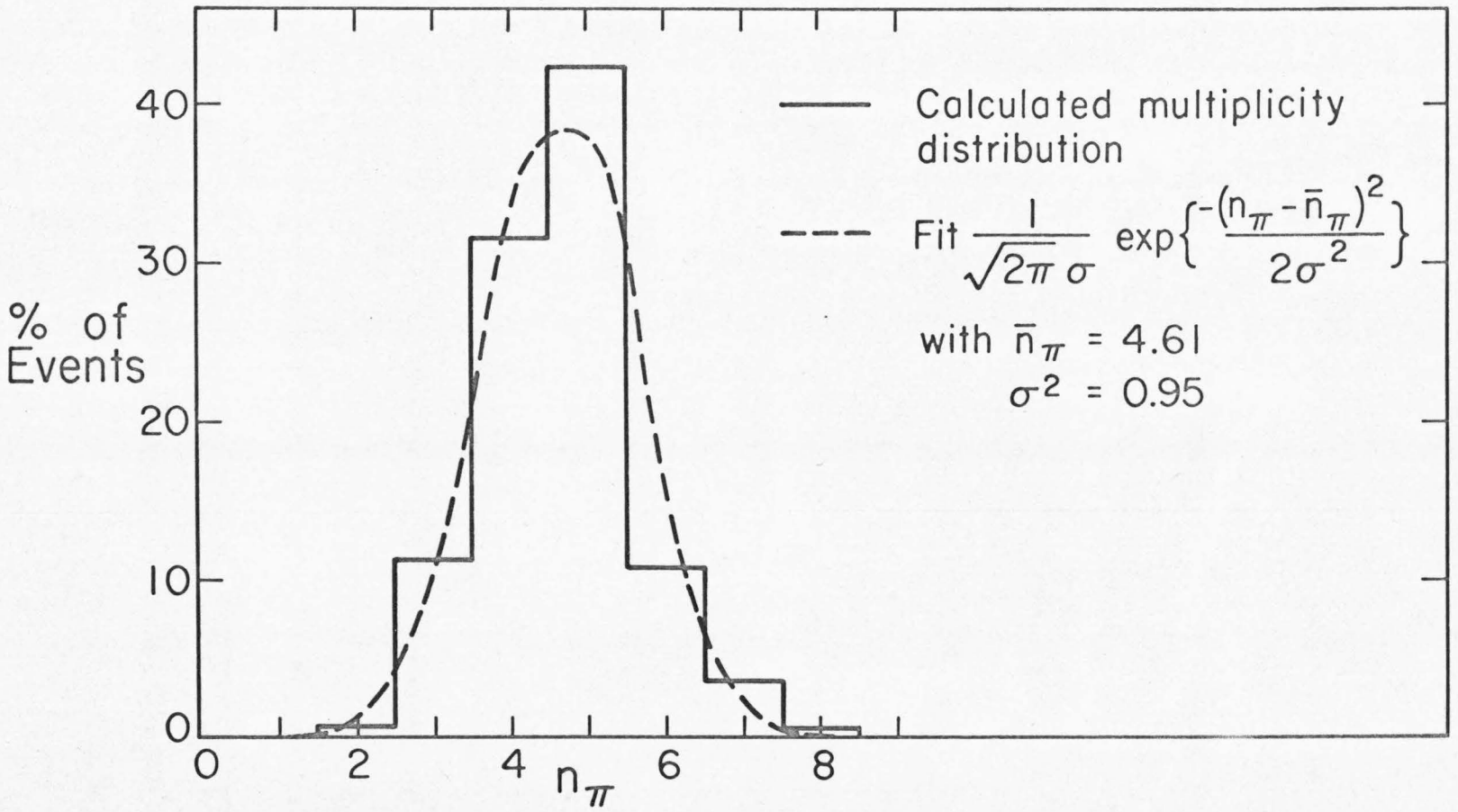

Figure 6. Calculated multiplicity distribution of pions in non-strange final states of $\bar{p}p$ annihilations. Also shown is a Gaussian fit (dashed line). Box radius R = 1.6F.

1.2.3 Statistical Fluctuations

In the previous two Sections, a statistical model has been developed[29,35] which will apply to any hadronic reaction proceeding via an incoherent sum over direct channel resonances. The model parallels the compound nucleus theory of Bohr in nuclear physics. Now it is an intrinsic feature of such a theory that the data must show statistical fluctuations, or deviations from the theoretically predicted average values. A search for these fluctuations in hadron physics has recently been made by Frautschi[35].

The magnitude of the fluctuations, and the distribution of the data about the mean, can actually be predicted on the basis of two assumptions:

i) That the resonance coupling constants to any single final state are determined by the chance values of many approximately independent dynamical variables, and behave like random numbers: that is, they are normally distributed about a mean of zero. This can only be assumed for resonances with identical quantum numbers, and all lying within the same small mass range* of order $\Delta m \lesssim m_\pi$; and less importantly,

---

*Compared to the scale on which the level density varies, for instance.

ii) That the resonance energies are distributed like the eigenvalues of a matrix whose elements are independent random variables.

The types of fluctuation which may occur can be categorized according to the energy region under consideration, as follows:

a) Separable resonance region. At these energies, the resonances can be separated from each other, and studied individually. As in the nuclear physics case, one would like to form distributions of level widths and spacings, and see whether they follow statistical laws. But unfortunately one runs into a familiar problem at this point: the hadron resonance widths are too large (of order $\Gamma \simeq m_\pi$). In order to test the statistical predictions, one needs a sizeable sample of resonances within a single small energy interval $\Delta E \simeq m_\pi$, all with the same quantum numbers. But at energies such that this situation occurs, the overlap between the resonances has already made it impossible to sort out one from the other. "The beautiful checks of statistical theory performed by nuclear physicists in the separable resonance region cannot be repeated in hadron physics"[35].

b) Overlapping resonance region. At energies high enough for resonances to overlap, one will still see peaks and dips in the reaction cross sections called "Ericson

fluctuations"[36]. In general it is not true that a single resonance is responsible for each peak, and instead the variations must be regarded as resulting from fluctuations in the number and coupling strength of all the overlapping resonances.

A quantitative measure of the Ericson fluctuations is provided by the correlation function:

$$C = \left\langle \frac{(\sigma[E] - \langle\sigma\rangle)^2}{\langle\sigma\rangle^2} \right\rangle \tag{1.34}$$

where $\sigma[E]$ is the cross section at energy E, and the brackets $\langle\rangle$ denote an average value taken over an energy range large compared to the fluctuation length. Now usually there will be some degree of coherence between the resonance contributions*, so the reaction amplitude must be written as the sum of a coherent term and a fluctuation term which averages to zero:

$$A = A^C + A^F \tag{1.35}$$

$$\text{Therefore } \langle\sigma\rangle = \langle|A^C + A^F|^2\rangle = |A^C|^2 + \langle|A^F|^2\rangle \equiv \sigma^C + \sigma^F \tag{1.36}$$

and hence one finds

$$C = \frac{(\sigma^F)^2 + 2\,\sigma^C\,\sigma^F}{(\sigma^F + \sigma^C)^2} \tag{1.37}$$

*Or perhaps an extra, non-resonant term.

Then σ^F and σ^C can be deduced from the data with the aid of Equations (1.36) and (1.37).

Now by a general result of statistical theory, the relative size of the fluctuations is proportional to $1/\sqrt{N}$, where N is the number of resonances contributing to the cross section at a given energy, i.e.

$$N \simeq \Gamma \rho(E) \tag{1.38}$$

where ρ is the density of resonant states and Γ is their average width. In cases where only direct channel resonance terms contribute, this means that

$$\frac{\sigma^F}{\sigma^C} \propto \frac{1}{N} \tag{1.39}$$

Since $\rho(E)$ goes up exponentially at large E, the fluctuation cross-section σ^F should die away very rapidly, like $e^{-\beta_0 E}$.

Frautschi[35] has discussed two types of reaction where one finds direct channel resonances, and where bumps appear at intermediate energies which might be interpreted as Ericson fluctuations*. The question is whether these bumps behave as expected according to the statistical bootstrap.

---

*The first searches for Ericson fluctuations in hadron physics gave negative results[37]. But the searches were made in experiments on pp elastic scattering, where there seem to be no direct-channel resonances anyway: this is the wrong place to look.

The cases are:

i) $\pi^{\pm}$ p elastic scattering at 0° and 180°, from 2 to 5 GeV/c. Here the experimental data are good. But the coherent term in the amplitude is large for elastic scattering, so the fluctuations are relatively small. Nevertheless, it can be seen that they behave very much as expected. The relative fluctuations are largest where the cross-section (σ^C) is small, as in the backward direction; and they die away rapidly at high energy. Frautschi[35] demonstrates that their size is quantitatively consistent with the statistical bootstrap theory, but the parameters in the model are not well enough known to make this a definitive test.

ii) K^-p backward scattering, from 2 to 5 GeV/c. In this reaction only exotic Regge pole exchanges can occur, and the leading Regge cut term is small[38]. Hence the coherent terms are small, and the cross-section may be dominated by the fluctuation term σ^F. A behavior $e^{-\beta \circ E}$ does in fact describe the average cross-section very well[25] [Figure 7]. But the data are too poor to tell whether the individual fluctuations are as large as expected, or not.

1.2.4 High-energy Hadronic Collisions

Applications of the thermodynamic or statistical bootstrap model in this area were pioneered by Hagedorn[9]. He and his collaborators (especially J. Ranft and G. Ranft)

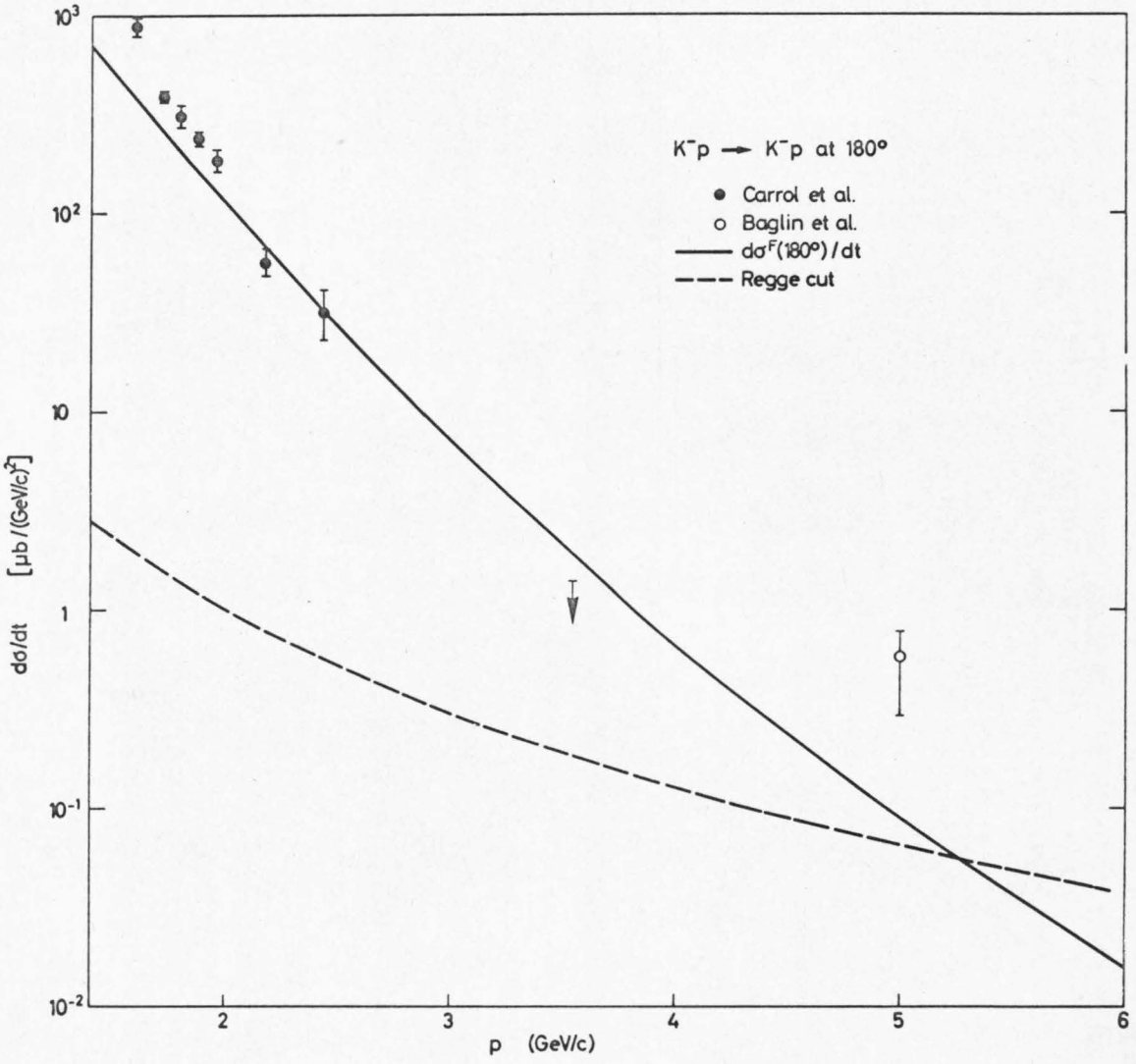

Figure 7. Cross-section for $\bar{K}p$ backward scattering, compared with statistical bootstrap prediction (solid line). From Frautschi, Ref. 35.

have elaborated on the subject in a series of papers[9, 14, 39] over the past several years, and performed many detailed fits to high energy data. We cannot recount the results in detail, but a summary of the principal assumptions and results will now be presented.

Hagedorn pictures the incoming particles as two blobs of hadronic matter, which collide as shown in Figure 8 in such a way that afterwards one finds a distribution of "hot" hadronic material moving with various velocities in the longitudinal direction. It is assumed that no "turbulence" occurs, i.e. that no transverse momentum is exchanged during the collision. The distribution of longitudinal velocities is taken as an empirical input in this model.

The hadronic matter "heated" in the collision by the conversion of kinetic energy then decays by emission of particles, in just the way described in Section (1.2.2). Hagedorn uses the methods of thermodynamics (i.e. the canonical ensemble) rather than phase space (the micro-canonical ensemble) in order to discuss this process, but the basic results are the same. The important physical consequences are as follows:

a) Limited transverse momenta. Given the initial assumption that no transverse momentum is produced in the original collision, the only way that the reaction products can acquire it is via their "thermal" motion inside the

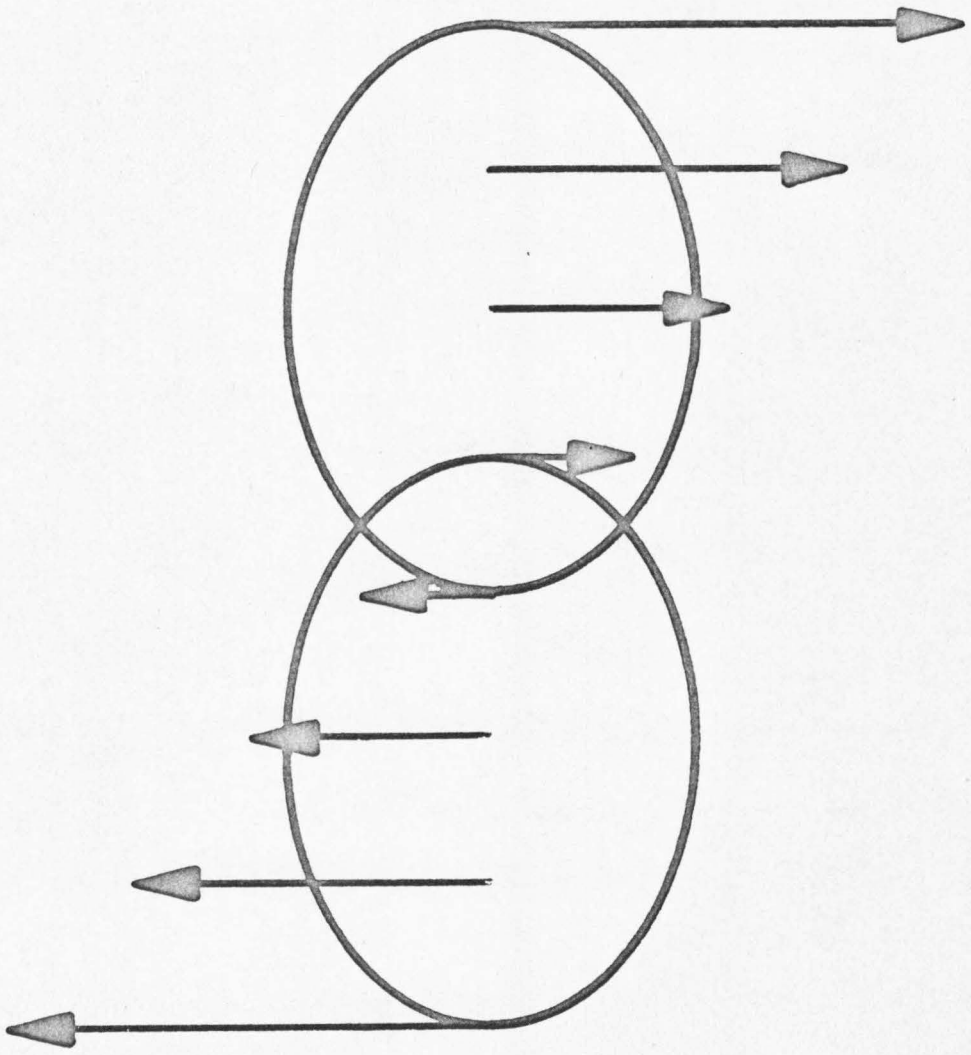

Figure 8. A high-energy hadron collision (thermodynamic model).

heated blobs. The distribution of transverse momenta should look like a projection of Equation (1.31), and cut off exponentially at large momenta. Empirical fits of this type to high-energy data work rather well. They give a value for the parameter T_{eff} of around 160 MeV[9,40], which is quite compatible with our result from $N\bar{N}$ annihilation - see Section (3.2).

b) Production rates for heavy particles. Here again, the rule is that the probability of a given particle carrying off a large energy is exponentially cut off. So the probability of producing a given heavy particle (or particle pair) decreases exponentially with its mass.* Hagedorn[14] has calculated the production rates for $\bar{K}$, $\bar{p}$, $\bar{d}$ and even $\overline{He^3}$ particles on this basis, and they agree well with experiment[41] [Figure 9], even though the results vary over about 10 orders of magnitude altogether!

The fact that experiment bears out the two predictions above provides further strong, though indirect, evidence for the exponentially rising density of states in the statistical bootstrap scheme.

It has recently become apparent, however, that Hagedorn's approach is open to criticism on one or two points of detail. First, he has taken the power a in the

*Thus Hagedorn[14] predicts that if the quark has a mass $\gtrsim 4m_p$, it is unlikely ever to be seen in an accelerator because the production rate will be too low.

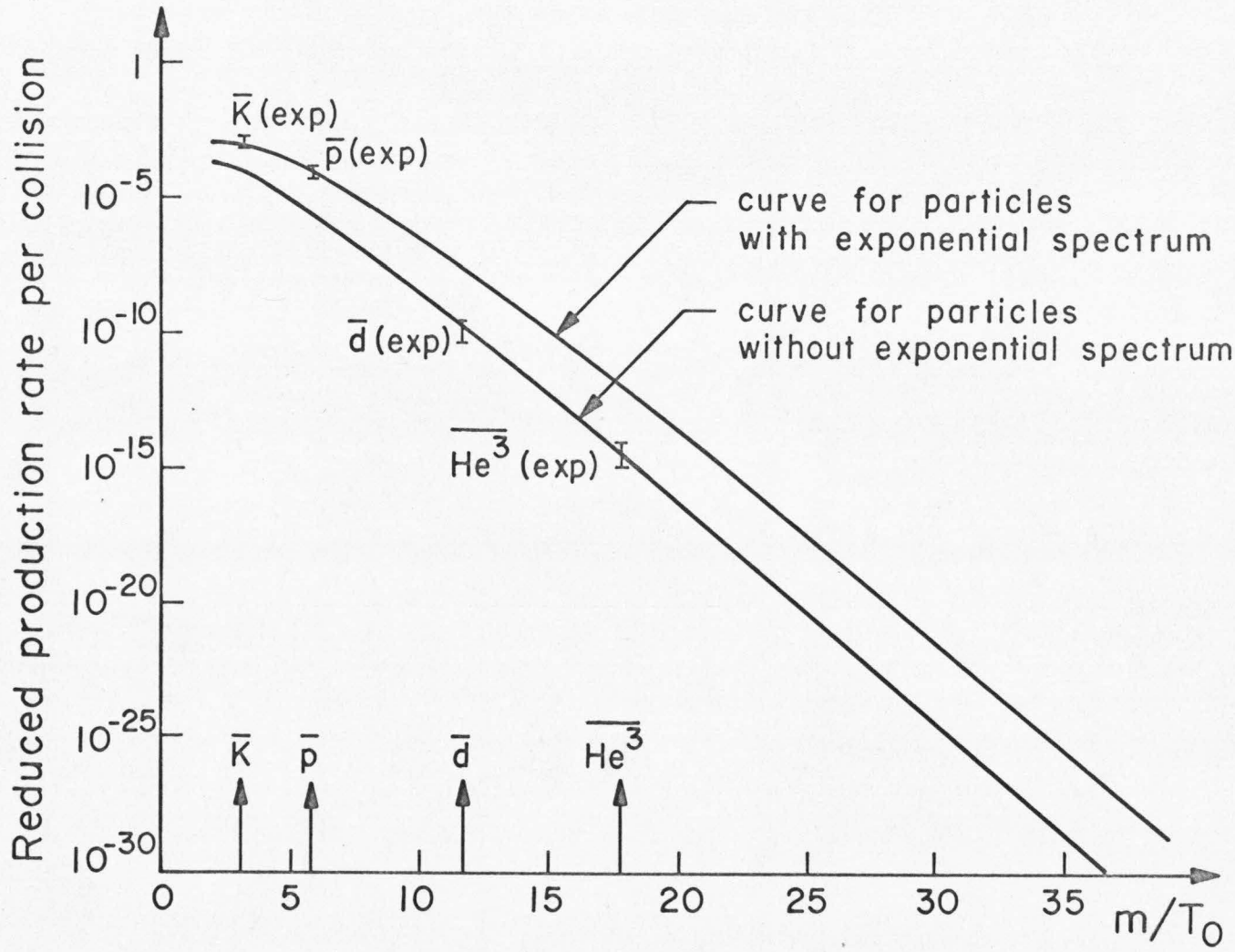

Figure 9. Production rates for heavy particles, compared with thermodynamic model predictions. From Hagedorn, Ref. 34.

mass spectrum to be -5/2 instead of -3. And second, it has been shown by Carlitz[42] that if a is in fact taken to be less than -5/2, then a thermodynamical treatment can lead to wrong results: the canonical ensemble gives different answers from the microcanonical ensemble (i.e. the phase space approach).* Thus the thermodynamic model may need some revision; but its two main consequences above will not be affected.

If we may be forgiven a moment of speculation, it is worth mentioning an alternative line of investigation here, namely the "multiperipheral cluster model" of high-energy collisions[43]. In this viewpoint, one regards the cross-section as the sum of a series of partial cross-sections as shown in Figure 10, where each square box represents the production of a "cluster". Each cluster is a collection of particles with low relative momenta, and may be assumed to result from the incoherent formation and decay of resonant states in a manner which should be capable of a statistical bootstrap description (as in Section [1.2.2]). In order to reach a mathematical formulation of the model, one would then have to deduce or assume expressions for the average

---

*This interesting state of affairs is apparently connected with the inhomogeneity of the system: for instance, the unsymmetrical result that for a $<-5/2$ one constituent likes to be heavy and all the rest light.

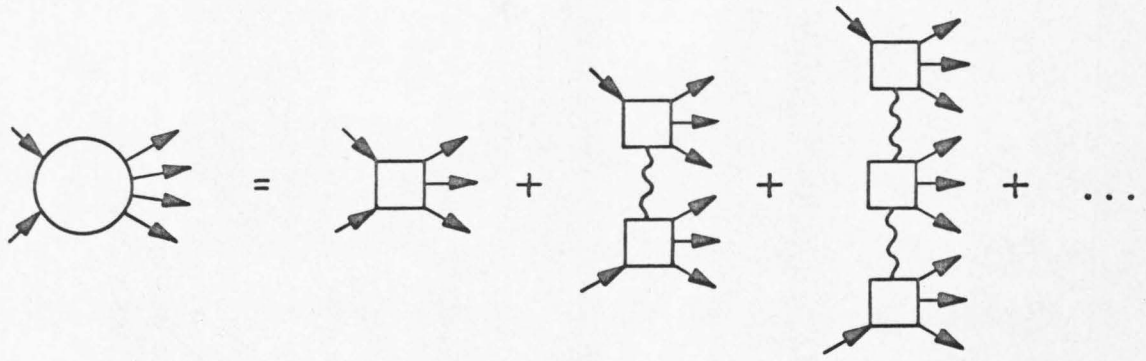

$$\sigma = \sigma_1 + \sigma_2 + \sigma_3 + \ldots$$

Figure 10. Multiperipheral cluster model of a high-energy hadron collision.

couplings at the vertices where the clusters are produced, and the (Reggeized?) dependence of the partial cross-sections on the various subenergies and momentum transfers. We have no such detailed formulation, nor any specific results to present, but we can enumerate some points in favor of the scheme.

a) Relation to Hagedorn's thermodynamic model. The two pictures are essentially Fourier transforms of each other: one deals in terms of impact parameters and configuration space (Figure 8), and the other uses momentum transfers and momentum space (Figure 10). The advantage of the cluster model are:

i) It is more convenient for the description of a process via phase space, and thus avoids the thermodynamic calculational techniques shown to be invalid by Carlitz[42];

ii) It allows one to incorporate the effects of energy and momentum conservation, which are neglected in the thermodynamic approach;

iii) It provides a popular and plausible explanation for the longitudinal momentum correlations, via the multiperipheral exchange mechanism, whereas in the thermodynamic model the correlations had to be accounted for by seemingly *ad hoc* assumptions. The implied connection between the two mechanisms has already been investigated by Ranft and Ranft[44].

A drawback is likely to be the increased difficulty of making calculations, but since we are only waving hands at the moment that problem can be ignored.

b) Relation to the ordinary multiperipheral model.

In any multiperipheral scheme, one has to answer the two basic questions [45]: what is exchanged, and what is produced at the vertices? We have no new answers to the first question, and it is likely to prove just as vexing as ever. But let us consider the second one carefully.

In the usual forms of multiperipheral model, one considers only the production of quasi-stable final state particles at each vertex, such as pions or occasionally ρ-mesons. It is recognized that the true multi-Regge kinematic region in which this provides an accurate description of the scattering process contains only a small fraction of all possible events: elsewhere the cross-sections exhibit the usual resonance bumps. But the pions hope is expressed that the treatment will also provide a reasonable average description even in the resonance region. This assumption rests on the principle of "duality"[46]: the idea that Regge exchanges and direct-channel resonance terms provide equally good alternative descriptions, on the average, for at least the imaginary part of a non-diffractive amplitude.

But the argument fails because we are dealing with cross-sections and not amplitudes. Consider, for example, the famous amplitude $\mathrm{Im}[A'^{(-)}]$ occurring in πN charge exchange scattering. As shown by Igi and Matsuda, and Dolen, Horn and Schmid[47], the Regge term does provide a good average description of the amplitude even in the low-energy region where isolated resonance bumps appear:

$$\mathrm{Im}[A'^{(-)}] = \mathrm{Im}[A_{\mathrm{Regge}}] + \mathrm{Im}[\delta A] \tag{1.40}$$

where δA is a term fluctuating about zero (Figure 11a). But when one squares the amplitude to form a differential cross-section one finds

$$[\mathrm{Im}A'^{(-)}]^2 = [\mathrm{Im}A_{\mathrm{Regge}}]^2 + [\mathrm{Im}\delta A]^2 + \begin{pmatrix}\text{interference terms}\\ \text{averaging to zero}\end{pmatrix} \tag{1.41}$$

and at energies up to 2 GeV or so it is the fluctuation term $[\mathrm{Im}\delta A]^2 \simeq \sigma^F$ which is of paramount importance (Figure 11b). This term is left out of the ordinary multiperipheral model, which therefore badly underestimates the importance of resonance production at low and intermediate energies. On the other hand, it is just such fluctuation terms which we may hope to describe via the statistical bootstrap model (see Section [1.2.3]), by introducing the "cluster" concept.

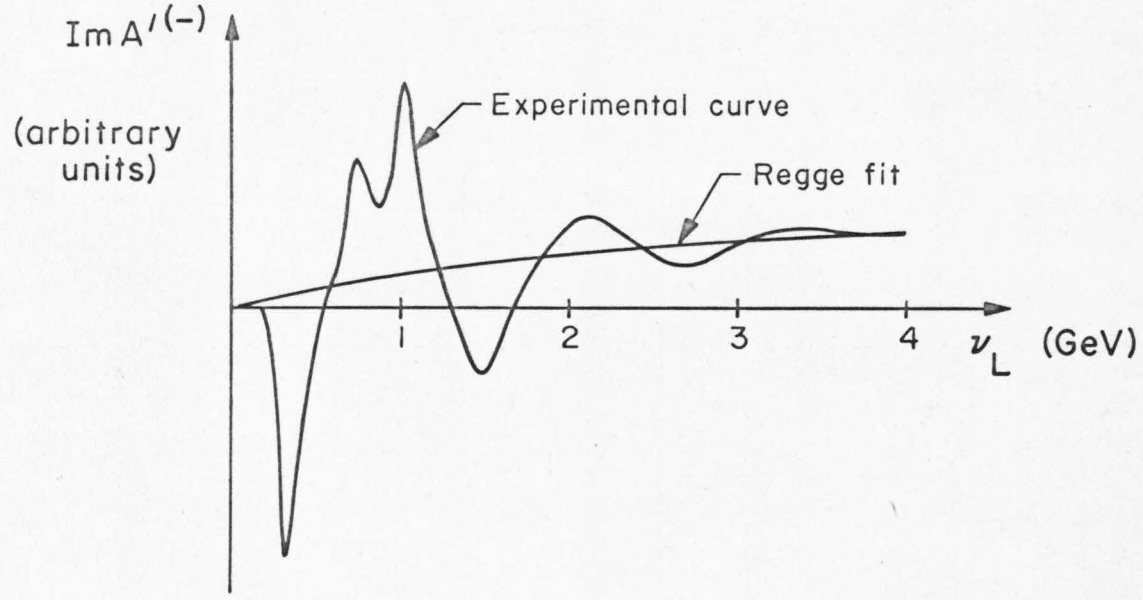

Figure 11 a) The amplitude $ImA'^{(-)}$ at t=0 in πN charge exchange scattering, and Regge fit.

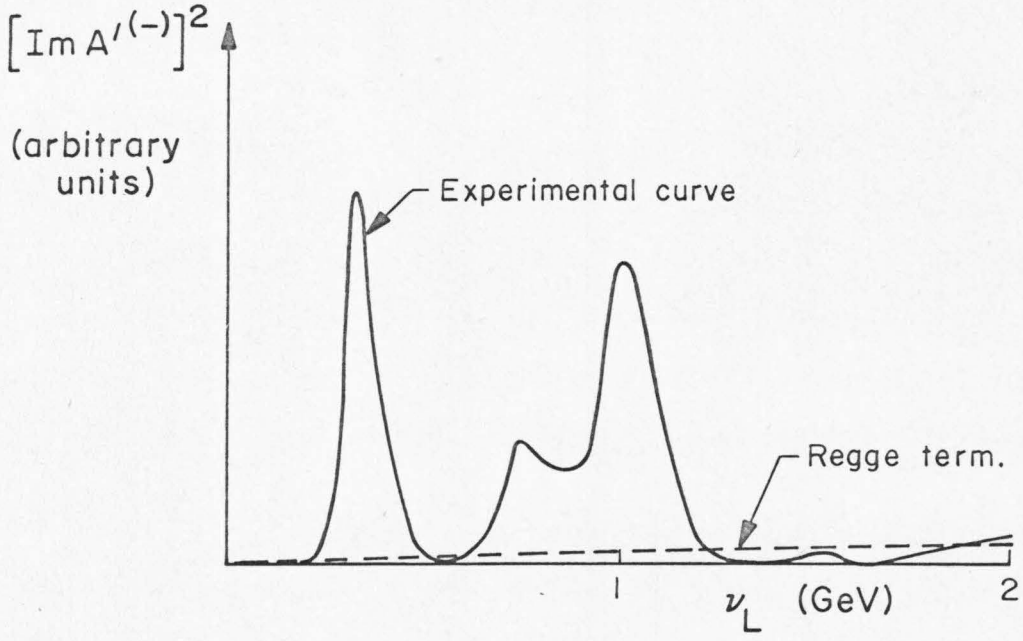

b) $[ImA'^{(-)}(t=0)]^2$ for πN CEX, and Regge term.

Phenomenologically, the need for such a modification has been evident for quite some time. The ordinary multiperipheral models tend to underestimate the importance of resonance production, to give low final-state multiplicities*, and to require unusually large Regge couplings, when compared with experiment. All these quantitative defects ought to be repaired in the cluster model.

Qualitatively, however, the new model should not produce any great surprises. Provided only that the rather peculiar term σ_1 of Figure 10 (corresponding to "central collisions") dies away fast enough with energy, the features of the model are likely to include: scaling at high energy, and logarithmic increase in multiplicities, as in the multiperipheral model; plus limited transverse momenta; plus exponential decrease in probability of producing heavy particle pairs, as in the thermodynamic model.

1.2.5 Other Applications

A very different field is which the high-mass hadron spectrum is relevant occurs in astrophysics. There one

---

*c.f. the situation in $N\bar{N}$ annihilation at rest before the advent of the statistical bootstrap model (Section [1.2.1]).

comes upon macroscopic states of very high density, for example in the big bang and in the interior of neutron stars. The questions which have been investigated include:

a) Quark production. According to current cosmology, "the universe cools as it expands following the big bang, from temperatures that exceeded 1 MeV during the first second. If the spectrum of particles did not rise exponentially, the temperature would rise higher and higher as we proceed back into the first second, eventually reaching the ionization point where matter dissociates into its quark constituents (if such a point exists). If there was once a phase when quarks dominated, quarks would still be quite numerous today because the subsequent cooling was too fast to allow all quarks to find each other and annihilate. Zeldovich[48] has estimated quarks would be about as common as gold, which is clearly contrary to observation.

If the spectrum rises like $\rho \sim e^{\beta_0 m}$, a different scenario is obtained. The temperature never rises above 160 MeV, and quarks do not necessarily become numerous."[49]

b) Equations of state. In a star which has condensed to nuclear densities or beyond, such as a neutron star, it will become possible to form excited resonant states, and the hadron level density becomes important in determining the equations of state for matter within the star. For

details, we refer the reader to Hagedorn's review[34], and to Frautschi, Bahcall, Steigman and Wheeler[50].

These applications can hardly be said to provide a test of the statistical bootstrap model. In fact, they must be regarded for the moment mainly as interesting speculations, because it is hard to come by experimental evidence which will either confirm or deny the hypotheses.

1.3 Summary

The basic feature of the statistical bootstrap model is the hypothesis that at high energies all reaction channels are to be treated on the same footing statistically, whether they contain "stable" constituents or unstable resonances. The validity of this hypothesis rests on the Beth-Uhlenbeck formula and the "narrow resonance" approximation.

The hypothesis has been applied in treatments of both the formation and decay of heavy resonances, and it leads to an exponentially rising density of states $\rho(m) \sim cm^{-3} e^{\beta_0 m}$. Now since the resonances have appreciable widths, and soon become densely distributed in energy, it rapidly becomes very difficult to distinguish one from the other by experiment. Thus it is impossible to verify the level density formula by a direct count. In fact, at high energies the very concept of a resonance must reduce to that of a more

or less hypothetical intermediate state in a reaction process, rather than that of an independent "particle".

The experimental evidence in favor of the model therefore comes almost entirely from reaction processes. There are several characteristic predictions of the statistical bootstrap which agree quantitatively with data. They are:

a) Limited transverse momenta. The exponentially rising density of states leads immediately to an exponential cut-off in the kinetic energies of reaction products. In Hagedorn's model of high-energy reactions[9], this results in limited transverse momenta: one of the most important and general features of the experimental results. The only point which needs further elucidation is why no large transverse momenta are generated in the initial (non-statistical) reaction mechanism.

b) Production of heavy particles. The statistical competition from other heavy particles implies that the probability of production of a heavy particle in a high-energy reaction drops off exponentially with its mass. Hagedorn[14] has shown this to be true for particles ranging from kaons to $\overline{He^3}$, with production probabilities ranging over 10 orders of magnitude (Figure 9).

c) Statistical fluctuations. As the level density rises, the relative magnitude of statistical fluctuations should decrease in the same exponential fashion. This has been verified by Frautschi[35] in some typical cases.

d) Final-state multiplicities. Conjugate to the prediction of low kinetic energies for reaction products is the prediction of high final-state multiplicities. Experimentally, the multiplicities are so high as to be an embarrassment to earlier statistical models, but they can be quantitatively explained in the statistical bootstrap[29].

e) Two-body final state branching ratios. The low values of the branching ratios into specific two-body final states in $N\bar{N}$ annihilation at rest were also an embarrassment to earlier statistical models. But they can be explained in the statistical bootstrap as the result of statistical competition between the exponentially rising number of reaction channels[29]. This feature should also be encountered in other reaction processes.

Taken together, these successful predictions form a very solid body of evidence in favor of the initial hypothesis.

There remains a good deal of work to be done in integrating a statistical model such as ours with a proper theory relating to the coherent terms encountered in high-energy reaction amplitudes. We have allowed ourselves some speculations as to how this might be done.

The only foreseeable alternative to a statistical approach such as the above in high-energy reactions consists of some generalized form of dual resonance model. Here too the level density rises exponentially, so that many of the features listed above might be reproduced (although as far as we are aware no such general predictions can yet be extracted from the model). The major difference is that everything is "coherent" in the dual resonance model. What we have called "fluctuations" would disappear even more rapidly with increasing energy; too rapidly in fact to explain the $K^- p$ backward scattering data* considered by Frautschi[35]. Even if the dual resonance model were true as some sort of first approximation, one would expect perturbations and configuration mixing to "randomize" the levels at high energies.

*This comment is due to C. Michael.

II. THE RESONANCE SPECTRUM

In this Chapter, we shall give proofs and demonstrations of the results summarized in Section 1.1 of the Introduction.

2.1 Asymptotic Form for the Level Density

A unique asymptotic form for the density of states was recently derived by Nahm[13]. A slightly simplified version of his treatment follows.

The basic equations we have to deal with are:

$$\rho_{out}(m) = \sum_{n=2}^{\infty} (V/h^3)^{n-1} \frac{1}{n!} \prod_{i=1}^{n} \int dm_i \; \rho(m_i) \int d^3p_i \; \delta\left(\sum_{i=1}^{n} E_i - m\right) \; \delta^{3)}\left(\sum_{i=1}^{n} \vec{p}_i\right) \quad (1.4)$$

$$\rho(m) \equiv \rho_{in}(m) = \rho_{out}(m) + \rho_{\substack{\text{low-mass} \\ \text{input}}}(m) \quad (1.8)$$

The asymptotic form of $\rho(m)$ will be derived in the following steps:

a) After a slight modification of Equation (1.4) which does not affect the form of the solution, the right-hand side can be made to take the shape of an exponential series of convolution products in the constituent sub-energies.

b) A Laplace transformation of both sides turns the convolutions into ordinary products.

c) The transformed densities possess singularities in the inverse "temperature" plane. These singularities must be matched on left and right sides of the equation in order to satisfy Equation (1.8). This determines the asymptotic form of the solution, and provides a series of sum rules relating the parameters of the asymptotic form to V and the low-mass input spectrum.

To start with, we switch from the normal phase-space expression (1.4) to the so-called "covariant" phase-space of Srivastava and Sudarshan[5.1)]

$$\rho_{out}(m) = \sum_{n=2}^{\infty} (V/h^3)^{n-1} \frac{1}{n!} \prod_{i=1}^{n} \int dm_i \; \rho(m_i) \int d^3p_i \, (m_i/E_i) \; \delta\Big(\sum_{i=1}^{n} E_i - m\Big) \; \delta^3\Big(\sum_{i=1}^{n} \vec{p}_i\Big) \qquad (2.1)$$

The purpose of this change is simply to make the calculations easier (it gets rid of correlations between the level densities of the constituents and their velocities relative to the box). Its effects are minor, and will be summarized later on.

Then the density of single-particle states with four-momentum p inside the box is

$$\bar{\rho}(p) = V/h^3 \int \rho(m)\ m/E\ \delta(E - \sqrt{m^2 + \vec{p}^2})\ dm \qquad (2.2)$$

For two-particle states, one finds

$$\bar{\rho}_2(p) = (V/h^3)^2 \frac{1}{2!} \prod_{i=1}^{2} \int dm_i\ \rho(m_i) \int d^3p_i \left(m_i/E_i\right) x$$

$$\delta^3)(\vec{p} - \sum_{i=1}^{2} \vec{p}_i)\ \delta(E - \sum_{i=1}^{2} E_i) = \frac{1}{2!} \int d^4p_1\ \bar{\rho}(p_1)\bar{\rho}(p-p_1) \qquad (2.3)$$

$$= \frac{1}{2!}\ \bar{\rho}(p) * \bar{\rho}(p) \qquad (2.4)$$

where the star denotes a convolution product. Treating the higher terms in the series similarly, one obtains from Equation (2.1) that

$$\bar{\rho}_{out}(p) = \exp * \{\bar{\rho}(p)\} - \bar{\rho}(p) - \delta^4(p) \qquad (2.5)$$

where the exponential convolution is defined in the obvious way as a series of convolution products, with the zeroth order term defined as $\delta^4(p)$.

Next, integrate over (three -) momentum, to find the total density of states at a given energy:

$$\bar{\sigma}(E) = \int d^3p\ \bar{\rho}(p) \qquad (2.6)$$

Then (2.5) simply becomes

$$\bar{\sigma}_{out}(E) = \exp * \{\bar{\sigma}(E)\} - \bar{\sigma}(E) - \delta(E) \qquad (2.7)$$

Now Laplace transform both sides of this equation, to get

$$Z_{out}(\beta) = \exp \{Z(\beta)\} - Z(\beta) - 1 \qquad (2.8)$$

$$\text{where } Z(\beta) = \int_0^\infty \bar{\sigma}(E)\, e^{-\beta E}\, dE \qquad (2.9)$$

Notice that the exponential convolution transforms into an ordinary exponential function. The quantity $Z(\beta)$ is just the normal partition function used in thermodynamics, with the "temperature" $T=1/\beta$. In order that $Z(\beta)$ exist, it is necessary to show that $\bar{\sigma}(E)$ will not increase <u>faster</u> than exponentially with E - we refer to previous workers[9,10,13] for this proof.

We now apply the bootstrap condition; i.e. we set out to match $Z_{out}(\beta)$ and $Z(\beta)$ as closely as possible. First, it is possible to demonstrate the necessity for a <u>singularity</u> in $Z(\beta)$. Since $\bar{\sigma}(E)$ is positive definite, and so is $Z(\beta)$, it follows from (2.8) that

$$Z_{out}(\beta) > \tfrac{1}{2} Z^2(\beta) \qquad (2.10)$$

On the other hand, $\bar{\sigma}_{out}(E) \leqslant \bar{\sigma}(E)$, so

$$Z_{out}(\beta) \leqslant Z(\beta) \qquad (2.11)$$

It is not possible for both (2.10) and (2.11) to be true for arbitrarily large Z. Yet even that part of the partition function corresponding to a single particle in the box increases beyond limit as β tends to zero. Therefore $Z(\beta)$ must have a singularity at some positive value $\beta=\beta_o$, so that smaller values of β cannot be reached. In order to create such a singularity, the level density must increase exponentially with energy.

Furthermore, $Z(\beta)$ has to stay <u>finite</u> even at the singularity in order to satisfy Equations (2.10) and (2.11). Such is <u>not</u> the case for Hagedorn's original spectrum[9] $\rho(m) \sim cm^{-5/2} e^{\beta_o m}$.

The specific form of the bootstrap condition which we shall apply is as follows:

$$\bar{\sigma}(E) - \bar{\sigma}_{out}(E) = 0(e^{-\lambda E}\ \bar{\sigma}(E)), \text{ for some } \lambda>0 \qquad (2.12)$$

$$= \bar{\sigma}_{\substack{\text{low-mass}\\ \text{input}}}(E)$$

Since $\bar{\sigma}(E)$ increases like $e^{\beta_o E}$, this condition should cover all cases of physical interest: the "low-mass input" spectrum can even rise exponentially itself, provided the coefficient of the exponential is less than β_o. It follows from this condition that the function

$$H(\beta) = Z(\beta) - Z_{out}(\beta) = \int_o^\infty \bar{\sigma}_{\substack{\text{low-mass}\\ \text{input}}}(E)\ e^{-\beta E}\, dE \qquad (2.13)$$

is <u>regular</u> at $\beta=\beta_o$. Equation (2.8) can now be written

$$\exp\{Z(\beta)\} - 2Z(\beta) - 1 = -H(\beta) \tag{2.14}$$

This equation can be solved by trial.* We are interested in the asymptotic behavior of $\bar{\sigma}(E)$, which is determined by the behavior of $Z(\beta)$ in the neighborhood of β_o. So let us try the expansions

$$H(\beta) = \sum_{k=0}^{\infty} b_k s^k , \tag{2.15}$$

where $s = \beta - \beta_o$, and

$$Z(\beta) = \sum_{k=0}^{\infty} a_k s^k + s^{\frac{1}{2}} \sum_{k=0}^{\infty} c_k s^k \tag{2.16}$$

Substitute into Equation (2.14), and match powers of s term by term. The solution turns out to be:

$$b_o = H(\beta_o) = 2 \ln 2 - 1 \tag{2.17}$$

$$a_o = Z(\beta_o) = \ln 2 \tag{2.18}$$

$$c_o = -\sqrt{-b_1} = -\sqrt{-H''}\,(\beta_o) \tag{2.19}$$

$$a_1 = -c_o^2/3! = b_1/3! \tag{2.20}$$

...etc.

---

*At this point, we diverge from Nahm's treatment, which contains one or two points which are obscure to the present author.

The following comments on this solution are in order:

a) Mathematically speaking, one should now prove that this solution is unique, and that the series (2.15) and (2.16) are convergent in the neighborhood of s=0. We shall not give any formal proof. But once one is given a low-mass input spectrum, it is clear that one can generate a unique bootstrapped spectrum at higher masses by a process of iteration in Equations (1.4) (or 2.1). A numerical example[12] was shown in Figure 2; and the asymptotic form of this numerically generated spectrum is in good agreement with the predictions of the treatment above. So the solution works in practice.

b) It is by no means obvious a priori that $Z(\beta)$ must take the form (2.16). But the square-root singularity is unique in that upon multiplying Z by itself one gets only square-root singularities back again. This is essential in order to be able to cancel singular terms between $\exp\{Z(\beta)\}$ and $2Z(\beta)$ in Equation (2.14).

c) Taking the inverse Laplace transform, one finds that the function $\bar{\sigma}(E)$ has the asymptotic form

$$\bar{\sigma}(E) = \sum_{k=0}^{\infty} c_k' \, E^{-3/2 \, -k} \, e^{\beta_o E} \qquad (2.21)$$

$$\text{and } \rho(m) = \sum_{k=0}^{\infty} c_k'' \, m^{-3 \, -k} \, e^{\beta_o m} \qquad (2.22)$$

The value of β_o is determined by the rather special relation (2.17), which has the form of a "sum-rule": an integral over the low-mass input spectrum, with weight factor $e^{-\beta_o E}$, is equal to a fixed constant. Once β_o (or b_o) is determined, all the other coefficients $b_k (k>1)$ can be worked out - they depend solely on β_o and the low-mass input spectrum. The coefficients $\{a_k\}$ and $\{c_k\}$ are then determined in terms of the $\{b_k\}$.

It is now possible to deal with the original model using the normal phase space expression (Equation [1.4]), rather than the "covariant" one (Equation [2.1]). Nahm[13] shows that up to terms of order $0(E^{-1}\,\bar{\sigma}(E))$ both models have the same structure. The only difference is that where the "covariant" version uses a momentum density $\bar{\rho}(p)$ given by Equation (2.2), the normal model replaces this by

$$\rho(p) = V/h^3 \int \rho(m)\ \delta(E - \sqrt{m^2 + \bar{p}^2}\ )\ dm \qquad (2.23)$$

To summarize, then, the asymptotic form of the mass spectrum will be

$$\rho(m) \underset{m\to\infty}{\sim} cm^{-3}\ e^{\beta_o m} \qquad (2.24)$$

where β_o is determined by the sum rule

$$2\ \ln\ 2 - 1 = H(\beta_o) = \int_o^\infty dE e^{-\beta_o E}\ V/h^3 \int d^3p \int \rho_{\substack{\text{low-mass}\\ \text{input}}}(m)dm$$

$$\delta(E - \sqrt{m^2 + \vec{p}^2}\ ) \qquad (2.25)$$

and c is given by:

$$c = \left(\frac{h^2\beta_o}{2}\right)^{3/2} \frac{1}{2\pi^2 V} \sqrt{-H''(\beta_o)} \qquad (2.26)$$

Take the numerical example illustrated in Figure 2, for instance. Here the low-mass input consisted of a single neutral "pion", and the radius R was taken to be 1.3 fermi. Then from the sum rules* (2.25) and (2.26) we predict $\beta_o = 0.85$ and $c = 1.4$;** whereas the least squares fit gave $\beta_o = 0.77$ and $c = 1.1$. Allowing for the numerical methods and approximations used[12] (particularly the use of a discrete rather than a continuous spectrum), these figures agree reasonably well.

Finally, we note that quantum statistics have not been properly taken into account for cases when identical particles occur in the same state: we have used a Maxwell-Boltzmann factor 1/n! to weight these states, rather than the correct values 0 for fermions and 1 for bosons. It turns out that the effect of the statistics can be rather

---

*Modified in a trivial way because n=2 terms only are considered in Equation (1.4).

**Units throughout this work will be such that $\hbar = m_\pi = 1$, as already stated in the Introduction.

neatly included in the partition function approach (refer once more to Nahm's paper[13]), but in any realistic case the magnitude of the effect on the asymptotic spectrum is unimportant. We shall therefore save space by neglecting it.

2.2 Characteristics of the Solution

In the basic Equation (1.4), the total density of states at a given mass is written as a sum of terms for various numbers of constituents within the box of volume V. We would like to know how the constituents are distributed in number, mass and kinetic energy, since these distributions will describe the decay products of a massive resonance, according to the model of Section (1.2). These characteristics were investigated by Frautschi[10], whose treatment is followed below.

Consider for example the n=2 term on the right-hand side of Equation (1.4):

$$\rho_{out}^{n=2}(m) = \frac{V}{2h^3} \prod_{i=1}^{2} \int dm_i \, \rho(m_i) \int d^3p_i \, \delta(E_1 + E_2 - m) \, \delta^3)(\vec{p}_1 + \vec{p}_2) \qquad (2.27)$$

The momentum integrations can be done with the aid of the δ functions, giving

$$\rho_{out}^{n=2}(m) = \frac{\pi V}{4h^3m^4} \int_{m_0}^{m-m_0} dm_1\ \rho(m_1) \int_{m_0}^{m-m_1} dm_2\ \rho(m_2)$$

$$[m^2 + m_1^2 - m_2^2]\ [m^2 + m_2^2 - m_1^2]$$

$$\sqrt{\{[m^2 - (m_1 - m_2)^2]\ [m^2 - (m_1 + m_2)^2]\}} \qquad (2.28)$$

Substituting in the asymptotic form $\rho(m) = cm^{-3}\ e^{\beta_o m}$, changing to the variables $m_\pm = m_1 \pm m_2$, and using the symmetry between positive and negative m_-, we rewrite (2.28) as

$$\rho_{out}^{n=2}(m) = \frac{16\pi Vc^2}{h^3m^4} \int_{2m_0}^{m} dm_+\ e^{\beta_o m_+} \sqrt{m^2 - m_+^2} \int_{o}^{m_+ - 2m_0} dm_-$$

$$(m_+^2 - m_-^2)^{-3}\ \sqrt{m^2 - m_-^2}\ (m^4 - m_+^2\, m_-^2) \qquad (2.29)$$

The integral peaks exponentially at $m_+ = m_1 + m_2 \simeq m$, and is then proportional to $(m^2 - m_-^2)^{-3/2}$, which means $|m_-| \simeq m$ is favored by a power. Thus the sum of the constituent masses is nearly equal to the total energy m; and of these constituent masses, one tends to be large and the other small.

The contributions from higher n are also maximal when one mass is large and all others small. Thus one gets asymptotically

$$\rho^n(m) \underset{m\to\infty}{\sim} (V/h^3)^{n-1}\ \frac{1}{(n-1)!}\ cm^{-3}\ e^{\beta_o m} \prod_{i=1}^{n-1} \int dm_i \int d^3p_i\ \rho(m_i)$$

$$e^{-\beta_o E_i} \qquad (2.30)$$

The factor $1/(n-1)!$ comes from $1/n!$ times an n for the number of different constituents which may have $m_i \simeq m$. The level density for this single high-mass constituent contributes the factor $cm^{-3}\ e^{\beta_o m}$.

Equation (2.30) can be immediately rewritten in terms of the partition function:

$$\rho^n(m) \underset{m\to\infty}{\sim} cm^{-3}\ e^{\beta_o m}\ \frac{1}{(n-1)!}\ [Z(\beta_o)]^{n-1} \tag{2.31}$$

$$= cm^{-3}\ e^{\beta_o m}\ \frac{[\ell n 2]^{n-1}}{(n-1)!} \tag{2.32}$$

using Equation (2.18).

Hence the probability of finding n constituents in the box is just

$$P(n) = \frac{(\ell n 2)^{n-1}}{(n-1)!} \tag{2.33}$$

independent of mass. This peaks very strongly at low n. The average particle number is $\bar{n} = 1 + 2\ \ell n\ 2 = 2.4$.

As pointed out by Frautschi [10], the distribution (2.33) can be physically interpreted as a modified Poisson distribution in the (n-1) low mass particles, resulting from the fact that each is emitted independently of the others and carries off a negligible fraction of the total energy.

The factor contributed by each low-mass constituent to the n-body phase space is

$$Z(\beta_o) = V/h^3 \int dm'\ \rho(m') \int d^3p\ e^{-\beta_o E} \tag{2.34}$$

Approximating the energy by its non-relativistic form, this becomes

$$Z(\beta_o) \simeq 4\pi\, V/h^3 \int dm' \, \rho(m') \, e^{-\beta_o m'} \int p^2 \, dp \, \exp(-\beta_o \, p^2/2m') \tag{2.35}$$

The average kinetic energy* of one of the low-mass constituents is therefore

$$\langle K.E. \rangle \simeq \int_o^\infty \frac{p^4}{2m'} \, dp \, \exp(-\beta_o p^2/2m') \Big/ \int_o^\infty p^2 \, dp \, \exp(-\beta_o \, p^2/2m')$$

$$= 3/2 \; \beta_o^{-1} \tag{2.36}$$

which is the same as the $\frac{1}{2}kT$ per degree of freedom of classical thermodynamics. Furthermore, after performing the momentum integration in Equation (2.35), and substituting $\rho(m') = cm'^{-3} e^{\beta_o m'}$, one has

$$Z(\beta_o) = cV \left(\frac{2\pi}{h^2 \beta_o} \right)^{3/2} \int dm' \, (m')^{-3/2} \tag{2.37}$$

The average mass of the light constituents is therefore:

$$\langle m' \rangle = \int_{m_o}^{m} dm' \, (m')^{-1/2} \Big/ \int_{m_o}^{m} dm' \, (m')^{-3/2} \simeq (m/m_o)^{1/2} \tag{2.38}$$

(here for the first time the mass of the "parent" state becomes important, and must appear at the upper limit of the mass integral). This result is only approximate,

*A better estimate will be given in Section (3.2).

because the asymptotic form of the mass spectrum is not accurate at low masses. The fact that $\langle m' \rangle$ increases with the parent mass was pointed out by Carlitz[42]. The fraction of the total energy carried away by the light constituents nevertheless becomes insignificant at large m, as stated above.

Finally, let us consider a different aspect of the asymptotic density function, namely its dependence on the volume V. Now β_o is determined from Equation (2.25), and in this equation it is more appropriate to take the extreme relativistic limit rather than the non-relativistic one, because Equation (2.25) involves only the low-mass input spectrum. Then

$$2 \ln 2 - 1 = H(\beta_o) = V/h^3 \int dm\, \rho_{\substack{\text{low-mass} \\ \text{input}}}(m) \int d^3p\, e^{-\beta_o p}$$

$$= (\text{constant}) \times (V/\beta_o^3) \qquad (2.39)$$

So in the relativistic limit β_o is proportional to the radius of the box. This works very well as an approximate rule of thumb (see Hamer and Frautschi[12]). Similarly one finds the coefficient c is proportional to $V^{-2/3}$.

2.3 Quantum Numbers

So far we have ignored the fact that the resonances have quantum numbers, and dealt solely with the total

density of states. It is a relatively trivial matter to include multiplicative quantum numbers such as parity, G-parity, etc.: one expects that the asymptotic density of states will be evenly divided between the positive and negative eigenvalues. But for additive quantum numbers there are two alternative scenarios, depending on whether restrictions are placed on the allowed resonance eigenvalues, or not.

2.3.1 Unrestricted Eigenvalues

Suppose, for example, that the bootstrap states are distinguished according to their charge Q (an identical argument will hold for strangeness, or any other additive internal quantum number). Further suppose that the low-mass input spectrum is symmetrically distributed about zero charge: for argument's sake, suppose it consists of three "pions" with Q = +1, 0 and -1 respectively. An argument was given in Section (1.1) to show[12] that the bootstrap states can be seen as resulting from a process of stuffing pions into the box one by one, so that the charge of the resonances is built up by a random walk process and should follow a Gaussian distribution $\exp(-d\,Q^2/m)$. We shall now demonstrate that such a form satisfies the bootstrap equations.

Consider first the n=2 bootstrap for simplicity. The partition function $Z^{Q}_{out}(\beta)$ for states of charge Q is then given by

$$Z^{Q}_{out}(\beta) = \tfrac{1}{2} \sum_{Q_1=-\infty}^{\infty} Z^{Q_1}(\beta)\ Z^{Q-Q_1}(\beta) \tag{2.40}$$

Assume that the sum over Q_1 can be replaced by an integral:

$$Z_{out}(\beta,Q) = \tfrac{1}{2} \int_{-\infty}^{\infty} dQ_1\ Z(\beta,Q_1)\ Z(\beta,Q-Q_1) \tag{2.41}$$

and let $\tilde{Z}(\beta,P)$ be the Fourier transform of $Z(\beta,Q)$ with respect to charge. Then after transforming both sides of Equation (2.41) we get rid of the convolution in charge:

$$\tilde{Z}_{out}(\beta,P) = \tfrac{1}{2}\ \tilde{Z}(\beta,P)\ \tilde{Z}(\beta,P) \tag{2.42}$$

Upon adding in the n = 3, 4, 5 -- terms, one finds

$$\tilde{Z}_{out}(\beta,P) = \exp\{\tilde{Z}(\beta,P)\} - Z(\beta,P) - 1 \tag{2.43}$$

This equation has a form identical to Equation (2.8), and will be satisfied by a function of the same form as in Equation (2.16), but with β_o replaced by a function f(P). The function f(P) is then determined from the low-energy sum rule:

$$\tilde{H}(f(P),P) = V/h^3 \int dm\ \tilde{\rho}_{\substack{\text{low-mass}\\ \text{input}}}(m,P) \int d^3p\ e^{-f(P)E}$$

$$\equiv 2\ \ln 2 - 1 \tag{2.44}$$

Expanding $\tilde{H}$ in a Taylor series about P = 0, and matching both sides of Equation (2.44) term by term, one finds

$$f(0) = \beta_o \tag{2.45}$$

where β_o is given by Equation (2.25) once more; and

$$f''(0) = -\frac{\overline{Q^2}}{\bar{E}} \equiv -\frac{1}{2d} \tag{2.46}$$

where $\overline{Q^2}$ and $\bar{E}$ are the average charge squared and energy of the low-mass input states, weighted by the Boltzmann factor $e^{-\beta_o E}$ as in Equation (1.19).

Retaining only these first two terms* in the expansion of $f(P)$, one can now invert the transforms to find the asymptotic form of the density of states:

$$\rho(m,Q) \underset{m\to\infty}{\sim} cm^{-3}\, e^{\beta_o m} \sqrt{\frac{d}{\pi m}}\, e^{-d\,Q^2/m} \quad , \tag{2.47}$$

which is the solution we expected to obtain on physical grounds. Note that the assumptions made in the derivation are justified for small $Q^2 (<m/d)$; and that the total density of states (summed over charge) will have the same form as if charge were not present:

$$\int_{-\infty}^{\infty} dQ\ \rho(m,Q) \sim cm^{-3}\, e^{\beta_o m} \tag{2.48}$$

---

*The higher terms will be of negligible importance at large m, finite Q.

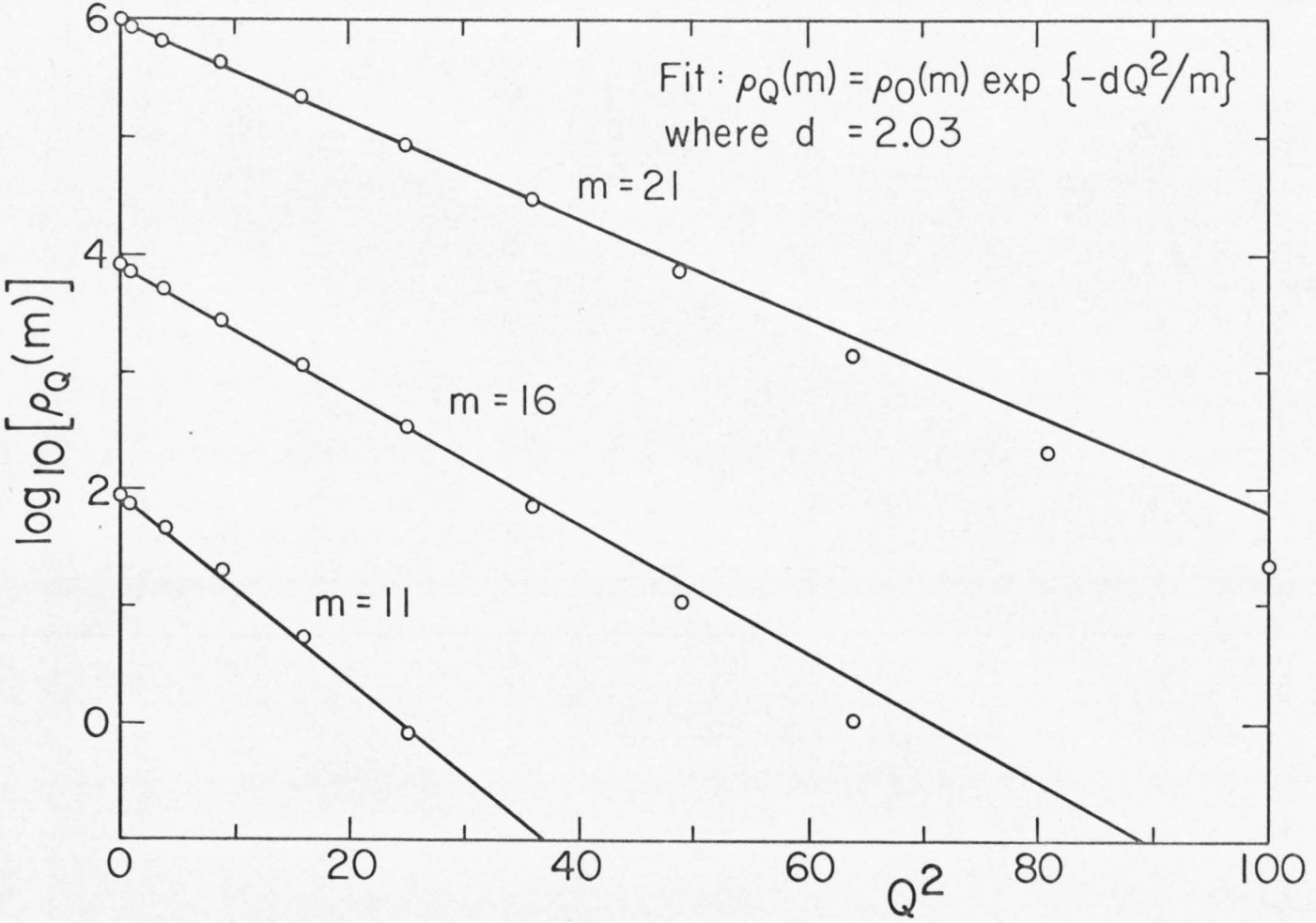

Figure 12. Density of states as a function of charge (circles), and fit to theoretical Q^2 dependence (straight lines), for the case discussed in Section (2.3.1).

A numerical example was worked out by Hamer and Frautschi[12]. The low-mass input consisted of three charged "pions" as above; the radius was taken as 1.3 fermi, and $n \leq 2$ terms only were counted in Equation (1.4). The resulting level density is displayed in Figure 12, together with a fit of the form of Equation (2.47). The values obtained in the fit for the parameters a, β_o, c and d compare with the predictions from Equations (2.25), (2.26), and (2.46) as follows:

	Prediction:	Fit:
a	-3	-2.9
β_o	1.18	1.15
c	1.2	1.3
d	2.22	2.03

The agreement is quite reasonable.

2.3.2 Restricted Eigenvalues

If only a finite list of eigenvalues is allowed, as in the case where no resonances are supposed to form in "exotic" channels, the results are somewhat different. Even the sum rules for the total density of states, Equations (2.25) and (2.26), need modification, because we have to throw away the states with exotic quantum numbers which would otherwise be present in the output density of

states, Equation (1.4). Such cases have been studied by Hamer and Frautschi[12], and by Nahm[13].

As a simple illustrative example, suppose that only states with Q = +1, 0 and -1 are allowed, and that the spectrum is symmetrically distributed with respect to charge. Consider the n = 2 bootstrap only.* Then the partition functions $Z^Q(\beta)$ will obey equations analogous to Equation (2.8).

$$\left.\begin{aligned} Z^{+}_{out}(\beta) &= Z^{\circ}(\beta)\ Z^{+}(\beta) \\ Z^{\circ}_{out}(\beta) &= \tfrac{1}{2}\ Z^{\circ}(\beta)\ Z^{\circ}(\beta) + Z^{+}(\beta)\ Z^{+}(\beta) \end{aligned}\right\} \qquad (2.49)$$

Now the same arguments as in Section (2.1) can be used to show that each partition function must have a singularity at some value $\beta = \beta_o$ (which must clearly be the same for both Z^+ and Z°). Expanding the partition functions in powers of $s = \beta - \beta_o$:

$$\left.\begin{aligned} Z^{+}(\beta) &= \sum_{k=0}^{\infty} a_k^{+}\ s^k + s^{\frac{1}{2}} \sum_{k=0}^{\infty} c_k^{+}\ s^k \ , \\ Z^{+}_{out}(\beta) &= \sum_{k=0}^{\infty} b_k^{+}\ s^k + s^{\frac{1}{2}} \sum_{k=0}^{\infty} c_k^{+}\ s^k \ , \end{aligned}\right\} \qquad (2.50)$$

*The addition of n = 3,4,5...terms will only produce minor quantitative changes in the results.

and similarly for Z° and Z°_{out}, then substituting in Equations (2.49), one finds that

$$c^{+}_{\circ}/c^{\circ}_{\circ} = 1/\sqrt{2} \tag{2.51}$$

and

$$[(a^{\circ}_{\circ} + \sqrt{2}\, a^{+}_{\circ}) - (b^{\circ}_{\circ} + \sqrt{2}\, b^{+}_{\circ})] = \tfrac{1}{2} \tag{2.52}$$

$$\text{i.e.} \quad H^{\circ}(\beta_{\circ}) + \sqrt{2}\, H^{+}(\beta_{\circ}) = \tfrac{1}{2} \tag{2.53}$$

In terms of level densities, this means that asymptotically

$$\rho_{Q}(m) \sim c_{Q}\, m^{-3}\, e^{\beta_{\circ} m} \tag{2.54}$$

so that the partial level densities are fixed in proportion to each other (with $c^{+}/c^{\circ} = 1/\sqrt{2}$), and $\beta_{\circ}$ is determined in terms of the low-mass input spectra by the sum rule (2.53).

In the general case, similar results will hold. If only a finite set of eigenvalues is allowed for any additive quantum number Q, then the partial level densities $\rho_{Q}(m)$ (summed over all other quantum numbers) will have a common asymptotic form $\rho_{Q}(m) \sim c_{Q} m^{-3}\, e^{\beta_{\circ} m}$, with the values $\beta_{\circ}$ and c_{Q} obtainable from the bootstrap equations by the means illustrated above.

2.3.3 Angular Momentum

Exploring the spin distribution of the bootstrap states is a rather more complex business than for internal quantum numbers. The constituents in the box have an orbital angular momentum $\vec{l} = \vec{r} \times \vec{p}$ which depends on their position and momentum relative to the center of mass, so it is not so easy to separate out the angular momentum dependence as it was for internal quantum numbers. Nevertheless the arguments and methods of Section (2.3.1) still apply, with only minor modifications.

The physical argument runs as follows. Each high-mass resonance is ultimately composed of a large number of low-mass particles placed into the box one by one with an average kinetic energy which is fixed and small. Therefore the average magnitude of the angular momentum contributed by each low-mass particle is also fixed and small. The total angular momentum of the high-mass resonance is therefore built up once again by a random walk process with a number of steps proportional to m; and the distribution in J_Z (where J_Z is the spin component in some arbitrary direction $\hat{Z}$ - an additive quantum number) should be a Gaussian, $\exp(-d\ J_Z^2/m)$. It has been shown by Chiu and Heimann[11] that a solution of this form will in fact satisfy the bootstrap equations. We use a modified version of their method.

The density of single-particle states in the box, summed over all momenta, can be written

$$\sigma(E) = 1/h^3 \int_V d^3 r \int d^3p \int dm\ \rho(m)\ \delta(E - \sqrt{m^2 + \vec{p}^2}) \qquad (2.55)$$

The density of states with angular momentum J_Z is then

$$\sigma(E,J_Z) = \int dJ_{1Z} \int dm\ \rho(m,J_{1Z}) \int d\ell_Z\ \phi(E,m,\ell_Z)\ \delta(J_Z - J_{1Z} - \ell_Z) \qquad (2.56)$$

where $\rho(m,J_{1Z})$ is the density of constituents with spin J_{1Z} at mass m, and $\phi(E,m,\ell_Z)$ is that <u>projection</u> of the single-particle phase space integral

$$\Phi(E,m) = 1/h^3 \int_V d^3 r \int d^3p\ \delta(E - \sqrt{m^2 + \vec{p}^2}) \qquad (2.57)$$

which ensures that the particle has orbital angular momentum ℓ_Z. Taking the Fourier transform of Equation (2.56) with respect to J_Z gives:

$$\tilde{\sigma}(E,\alpha) = \int dm\ \tilde{\rho}(m,\alpha)\ \tilde{\phi}(E,m,\alpha) \qquad (2.58)$$

where α is the conjugate variable to J_Z.

The projection technique involved in finding $\phi(E,m,\ell_Z)$ was invented by Cerulus[52]. The phase space integral Φ can be regarded as a count of momentum eigenstates inside the enclosure, weighted by their (uniform) spatial distribution upon performing the phase space integrals:

$$\Phi(E,m) = \frac{1}{h^3} \int_V d^3r \int d^3p \; \delta(E - \sqrt{m^2 + \vec{p}^2}) \; [e^{-i\vec{p}\cdot\vec{r}} \, e^{+i\vec{p}\cdot\vec{r}}] \quad (2.59)$$

When only states with a definite l_Z are to be counted, their spatial distribution is no longer uniform, and is obtained by projecting l_Z eigenstates from the momentum eigenstate $e^{i\vec{p}\cdot\vec{r}}$. Then

$$\phi(E,m,l_Z) = \frac{1}{h^3} \int_V d^3r \int d^3p \; \delta(E - \sqrt{m^2 + \vec{p}^2}) \; [e^{-i\vec{p}\cdot\vec{r}} \, P_{l_Z} \, e^{i\vec{p}\cdot\vec{r}}] \quad (2.60)$$

where the projection operator*

$$P_{l_Z} = 1/2\pi \int_{-\infty}^{\infty} d\phi \; e^{-il_Z\phi} \, e^{i\phi L_Z} \quad (2.61)$$

and $L_Z = -i \, \partial/\partial\phi$ is the operator for the Z-component of orbital angular momentum. This procedure is essentially a partial wave analysis.

Now when the angular momentum $l = \vec{r} \times \vec{p}$ is projected out, there is a coupling of the $\vec{r}$ and $\vec{p}$ dependences in ϕ, and the answer depends on the nature of the volume cut-off. A potential "box" has a sharp cut-off, of course; but Chiu and Heimann[11] assume a Gaussian cut-off instead, to facilitate their computations:

---

*The limits on this integral run from $-\infty$ to $+\infty$, rather than over a period 2π, because l_Z has been treated above as a continuous rather than a discrete variable.

$$\int_V d^3 \vec{r} \to \int d^3 r \; e^{-r^2/R^2} = (\sqrt{\pi}\, R)^3 \equiv V \tag{2.62}$$

The Fourier transform of ϕ can now be calculated[11]

$$\tilde{\phi}(E,m,\alpha) = 4\pi \, VpE \int_0^1 dZ \; e^{-R^2 p^2 c(\alpha)\,(1-Z^2)} \tag{2.63}$$

where $c(\alpha) = \frac{1}{2}(1-\cos\alpha)$. (2.64)

So the functions $\tilde{\rho}$ and $\tilde{\phi}$ in Equation (2.58) can now be calculated also.

The Laplace transform $\tilde{Z}(\beta,\alpha)$ of $\tilde{\sigma}(E,\alpha)$ will obey a bootstrap equation identical in form to (2.43), and its solution can be found by methods identical to those of Section (2.3.1). So the asymptotic density of states is

$$\rho(m,J_Z) \underset{m\to\infty}{\sim} cm^{-3} \; e^{\beta_0 m} \sqrt{\frac{d_J}{\pi m}} \; e^{-d_J J_Z^2/m} \tag{2.65}$$

where $d_J = \frac{1}{2} \dfrac{\overline{E}}{\overline{J_Z^2}}$ (2.66)

the quantities $\overline{E}$ and $\overline{J_Z^2}$ being averages over the low-mass input states at "temperature" T_0. For a Gaussian volume cut-off,

$$\overline{J_Z^2} = \overline{S_Z^2} + \overline{l_Z^2} = 1/3 \; \overline{S^2} + R^2/3 \; \overline{p^2} \tag{2.67}$$

where $\overline{S^2}$ is the average spin squared of the low-mass input states.

The number of resonances with total spin J at mass m is then[11]

$$\rho(m,J) \simeq - \partial \left. \frac{\rho(m,J_Z)}{\partial J_Z} \right|_{J_Z = J + \frac{1}{2}}$$

$$= cm^{-3} e^{\beta_o m} (2J+1) \sqrt{\frac{d_J^3}{\pi m^3}} e^{-d_J (J+\frac{1}{2})^2/m} \qquad (2.68)$$

Note that the average spin* goes like $\sqrt{m}$:

$$\langle J \rangle \simeq 2 \sqrt{\frac{m}{\pi d_J}} \qquad (2.69)$$

whereas in the Veneziano model $\langle J \rangle \propto m$.[53] So the detailed structures of the statistical bootstrap and Veneziano models are actually very different, in spite of the similarity in the behavior of the total level densities.

To give an idea of the order of magnitude of d_J, we have calculated it from Equation (2.66) for the case described in Section (2.3.1): low-mass input of a "pion" (I=1, J=0), radius 1.3 fermi. The result is $d_J = 0.66$.

Chiu and Heimann[11] actually found other solutions to the bootstrap besides the form (2.68), but they only applied

*After weighting each resonance state by the spin multiplicity factor (2J +1).

the bootstrap condition in the asymptotic region. Our stronger condition (1.8) establishes Equation (2.68) as the unique solution.

2.4 A Realistic Model

Hamer and Frautschi[12] have constructed a numerical model of the actual hadron spectrum, using the statistical bootstrap theory. Starting from a set of input states, the energy was raised step by step in intervals of m_π, which seemed a convenient unit. At each step, $\rho_{out}(E)$ was evaluated as the sum over all channels of the available phase space in the box of volume V, according to the right-hand side of Equation (1.4), and the appropriate increment was added to the integral $\int_0^E \rho_{out}(E')\, dE'$. Each time this integral was found to have risen by one, a state was added to ρ_{in} at that energy. In this way, a discrete spectrum of "bootstrapped" states was generated. The radius of the box was taken to be 1.3 fermi, which is a reasonable strong interaction radius.

Since the computation of the phase space contributions becomes rapidly longer and more complex as the number of constituents in the box increases, and since the dominant contributions come from channels with small numbers of constituents (Section [2.2]), we have cut off the sum in Equation (1.4) at n = 3 in the computer calculations. The

contributions from terms with higher n can be estimated with confidence[12], and are small* (they would produce an increase of about 2% in the value of β_o).

Finally, when the spectrum of states had been generated up to sufficiently high energy, least squares fits were performed to test whether the spectrum could be properly represented by the form $cm^a e^{\beta_o m}$. It turns out that the spectrum does rapidly approach a stable solution of this form, with $a \simeq -3$.

In order to exclude exotic states from the process, it was necessary not only to banish channels with exotic Q, S and B from consideration, but also to eliminate exotic SU(3) states (neutral members of I = 2 multiplets, etc.). This was achieved, in an average sense, by including Clebsch-Gordan coefficients in the bootstrap equations:

$$\rho^{\alpha}_{I,Y,B}(m) = \sum_{n=2}^{\alpha} (V/h^3)^{n-1} \frac{1}{n!} \prod_{i=1}^{n} \int dm_i \int d^3p_i \, \delta^3\left(\sum_{i=1}^{n} \vec{p}_i\right)$$

$$\delta\left(\sum_{i=1}^{n} E_i - m\right) \times \sum_{\substack{\alpha_i, I_i, Y_i, B_i \\ \alpha_i', I_i', Y_i'}} \rho^{\alpha_i}_{I_i Y_i B_i}(m_i) \begin{pmatrix} \alpha_i & \alpha_i' & \alpha_{i+1}' \\ I_i Y_i & I_i' Y_i' & I_{i+1}' Y_{i+1}' \end{pmatrix}^2$$

$$\times \, \delta\left(\sum_{i=1}^{n} B_i - B\right) \delta(I_{n+1}' - I) \, \delta(Y_{n+1}' - Y) \, \delta(\alpha_{n+1}' - \alpha) \, \delta(\alpha_1' - 1)$$

$$\delta(I_1') \, \delta(Y_1') \qquad (2.70)$$

*For a discussion of various errors and uncertainties in the calculations, we refer the reader to the original paper. The result is a net "error" of order 5% in the calculated value of β_o.

(This horrendous equation is handled relatively easily by the computer). The parameters α denote SU(3) representations, and the sums run over all non-exotic representations* (**1**, **8** and **10** for baryons, **1** and **8** for mesons). The SU(3) coefficients used are the "isoscalar factors" given by de Swart[54]. We have lumped together the two octets obtained in the Clebsch-Gordan series

$$\mathbf{8} \times \mathbf{8} = \mathbf{1} + \mathbf{8}_1 + \mathbf{8}_2 + \mathbf{10}^* + \mathbf{10} + \mathbf{27} \qquad (2.71)$$

Finally, we note that $\rho^{\alpha}_{IY}(m)$ denotes the density of SU(2) multiplets, so that the density of states will include an extra factor $(2I + 1)$.

First of all, the meson spectrum was generated. A realistic low-mass spectrum of SU(3) multiplets was fed in as input (all masses being taken to the nearest multiple of m_π). It was found that the $J^P=0^-$ nonet was not sufficient input, in that no resonances were generated at the position of the ρ; so the ρ nonet ($J^P=1^-$) was also taken as input. This squares with the quark model picture, in which the ρ multiplet is a spin partner of the π, not a spatial excitation.

---

*This actually implies a small error in the treatment of channels with n>2, since there is no reason why subgroups of constituents should not have exotic net quantum numbers as long as the combination of all of them is non-exotic. Our neglect of such terms should have only a small effect.

From there on, the bootstrap program was set free to run, and the meson spectrum was generated* up to a mass of $32m_\pi$.

Next, the baryon spectrum was generated. The whole [**56**, 0^+] baryon supermultiplet was taken as input, together with the previously calculated meson spectrum, and the bootstrap was set to run. For reasons of economy the spectrum was not generated beyond $26m_\pi$.

The results are displayed in Figures 13 and 14, which compare the spectra generated by the bootstrap with experiment, for each of the various isospin multiplets.

A comparison shows that the density of baryon states is increasing at a consistently higher rate than the meson density. The baryons multiply more rapidly at low masses, because the proportion of states generated by the bootstrap which have to be excluded as "exotic" is lower for baryons than for mesons. At higher masses, however, $B\bar{B}$ contributions to the meson spectrum will restore the balance so that in the asymptotic region the meson and baryon densities will rise at the same rate. This situation will not be reached until $m>50m_\pi$.

---

*We note in passing that the $\bar{B}B$ contribution to the meson spectrum was assumed negligible.

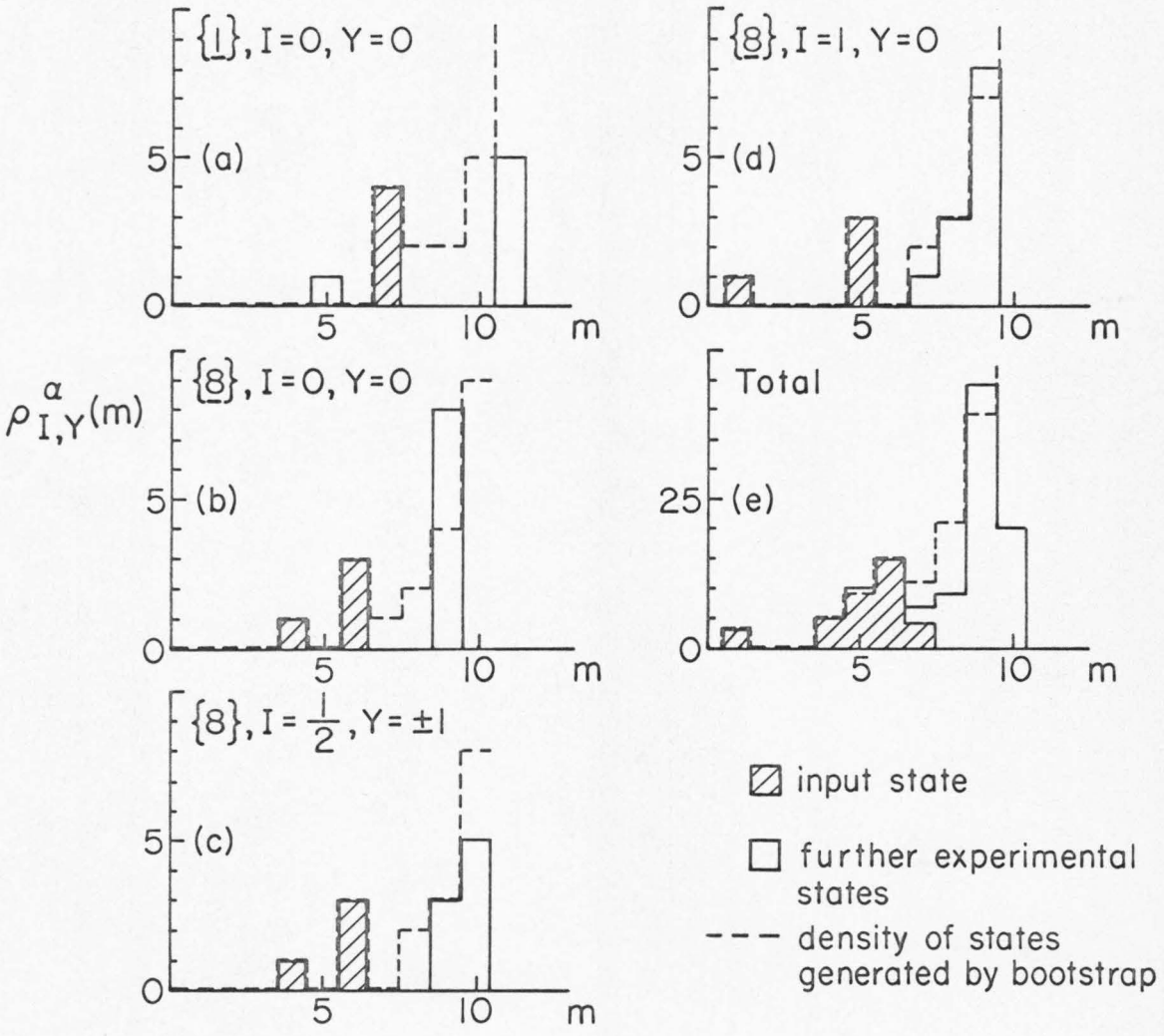

Figure 13. Comparison of bootstrap results with experiment for mesons (units $m_{\pi} = 1$). The experimental states are those listed by the Particle Data Group.[15] In Figures 13a)-d), the density of isospin multiplets is plotted; but 13e) shows the density of individual states.

Figure 14. Comparison of bootstrap results with experiment for baryons (units $m_\pi = 1$). The experimental states are those listed by the Particle Data Group[15]. In Figures 14a)-i), the density of isospin multiplets is plotted; but 14j) shows the density of individual states. The curves represent input states (shaded), further experimental states (solid line), and density of states generated by the bootstrap (dashed line).

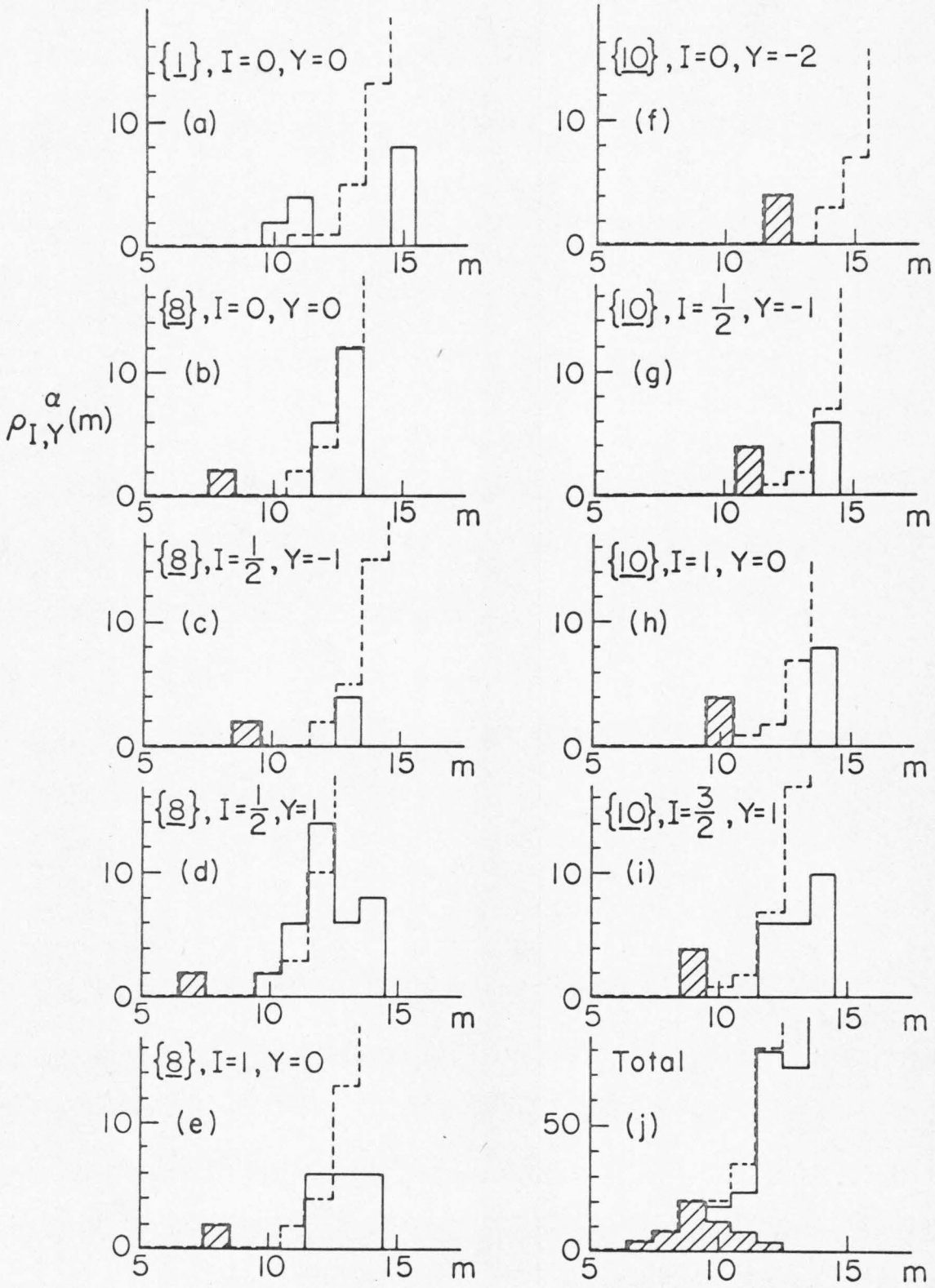
$\rho^{\alpha}_{I,Y}(m)$
{1}, I=0, Y=0
(a)
{8}, I=0, Y=0
(b)
{8}, I=1/2, Y=-1
(c)
{8}, I=1/2, Y=1
(d)
{8}, I=1, Y=0
(e)
{10}, I=0, Y=-2
(f)
{10}, I=1/2, Y=-1
(g)
{10}, I=1, Y=0
(h)
{10}, I=3/2, Y=1
(i)
Total
(j)
10
50
0
5
10
15
m

This means that it is only the baryon spectrum which can have approached its asymptotic form in the numerical results. A fit to this spectrum gives for all baryon states

$$\rho_{B=1}(m) \sim c_{B=1}\, m^{-3}\, e^{\beta_o m} \qquad (2.72)$$

where $\beta_o = 1.07 \pm .005$, which corresponds to a limiting temperature $T_o \simeq 132$ MeV for a box radius $R = 1.3$ fermi; and $c_{B=1} = 0.55 \pm 0.2$. This value of β_o is in good agreement with an analytical estimate by Nahm[13].

The asymptotic ratios between densities of states with various quantum numbers are shown in Table I. For the meson densities, we must rely on the analytical estimates made by Nahm[13], although these are only approximations, because the complications due to an irregular input spectrum and the SU(3) quantum numbers make it difficult to solve the bootstrap equations by the methods of Section (2.3).

Comments on these results have already been made in the Introduction. At this point, we merely note that no explicit mention has been made of angular momentum. In dealing with this aspect, a shape for the potential well has to be assumed, and the model has not reached such a stage of development that details of this sort are worth worrying about.

TABLE I

Asymptotic values for the proportions of each type of particle in the total density of states.

A. Baryons

	Type	Fraction (%)
{1}	I=0, Y=0	2.3
{8}	I=0, Y=0	5.9
	I=½, Y=-1	6.3
	I=½, Y=+1	21.2
	I=1, Y=0	21.8
{10}	I=0, Y=-2	0.6
	I=½, Y=-1	3.0
	I=1, Y=0	10.3
	I=3/2, Y=1	28.6

B. Mesons (from Nahm[13])

The ratios of SU(3) multiplet densities are approximately

$$\frac{\rho(\mathbf{8},\ B=0)}{\rho(\mathbf{8},\ B=1)} = 0.6; \quad \frac{\rho(\mathbf{1},\ B=0)}{\rho(\mathbf{8},\ B=1)} = 0.2$$

III. APPLICATIONS

In this Chapter a more detailed development is given of the subjects summarized in Sections (1.2.1) and (1.2.2) of the Introduction.

3.1 $N\bar{N}$ Annihilation at Rest

As outlined in the Introduction, we have modified Fermi's statistical model[26] for the annihilation process so as to take full account of resonance production, using the statistical bootstrap model. The resulting picture is similar to the compound nucleus model of nuclear reactions, and envisages the annihilation as taking place via a chain of resonance decays (Figure 4).

The statistical branching ratios for decay of one these "bootstrapped" resonances, in the first generation, can be read off almost immediately from the program used to calculate the "realistic" spectrum. The level density generated at a given mass is equal to the total phase space available, within V, to all the possible constituent states. So the branching ratio into any given combination of constituents is just the proportion of phase space contributed by that combination to the total. These first generation

reaction products will then decay in their turn, and so on down the chain; but the branching ratios into the various ultimate final states (with stable constituents only) can be simply deduced from those of the first generation decay products, assuming these are known. In practice, the decay modes of the input mesons were taken from the Particle Data Group tables[15], and then the decay modes of the resonances generated by the bootstrap were calculated for successively higher masses by the phase space prescription above.

The branching ratios for $N\bar{N}$ annihilation are assumed to be the same as those for the decay of meson resonances of the same mass and quantum numbers. Some assumptions were made about the relative probability of annihilation in various SU(3) channels, with the proportions being:

$$\bar{p}n = 1 \times [\mathbf{8},\ I=1]$$

$$\bar{p}p = 3/8 \times [\mathbf{8},\ I=1] + 5/8 \times \{8/13 \times [\mathbf{8},\ I=0] + 5/13 \times [\mathbf{1},\ I=0]\} \qquad (3.1)$$

The reasoning behind these figures is:

i) Desai[55] has shown that the Coulomb field will produce transitions between different isospin (and SU(3)) states of the $N\bar{N}$ system at a much more rapid rate than the occurrence of annihilation, so that it is possible to assume that annihilation only takes place via "non-exotic" SU(3) channels which are dominated by resonances;

ii) The evidence from $\bar{p}d$ annihilation processes[28] is that the ratio of the (I=0) to (I=1) rates is about 5:3, as used above. Lacking any further experimental information, we have also assumed that the ratio of [8, I=0] to [1, I=0] rates for $\bar{p}p$ is just equal to the ratio of the squares of the SU(3) isoscalar factors connecting the $\bar{p}p$ state to the SU(3) states in question.

Finally, G-parity selection rules have been approximately taken into account. For an $\bar{N}N$ state,

$$G = (-1)^{L+S+I} \tag{3.2}$$

and it is known that annihilations at rest occur predominately from S-wave states[56,28]*, so that in a given isospin channel the G-parity is determined by the spin. Since the electromagnetic spin-flip transitions in the $N\bar{N}$ system occur at a <u>slower</u> rate than annihilation[55], we assume that the ratio of singlet to triplet annihilations takes the statistical value of 1:3 which is appropriate to the initial formation of the $N\bar{N}$ bound state before annihilation. Then the branching ratios into final states containing even numbers of pions (G=+1) or odd numbers (G=-1), and with a given isospin, are multiplied by factors ½ or $^3/_2$ accordingly.

---

*Although this result has lately been called into question by Devons et al., *Phys. Rev. Letters 27*, 1614 (1971).

The $N\bar{N}$ branching ratios can now be calculated. It is worth noting that the results are open to several sources of error:

i) The assumptions as to internal quantum numbers which are outlined above are somewhat crude. Fortunately the results are not very sensitive to the treatment of SU(3) quantum numbers; but the G-parity selection rule will obviously have important effects.

ii) No account has been taken of angular momentum conservation. This would restrict the phase space available in any given channel, but it would also restrict the total phase space similarly[26], and the two effects tend to cancel each other out in the branching ratios.

iii) It turns out that there is a dynamical mechanism at work to suppress channels involving $K\bar{K}$ production[33], which has not been taken into account.

iv) Purely calculational errors and approximations may occur, such as were discussed by Hamer and Frautschi[12] in connection with the spectrum calculation.

Furthermore, one expects statistical fluctuations to be apparent in the data. Some consideration of this effect is necessary in order to judge our results, as emphasized by Frautschi[35]: it will be discussed more fully in Section (3.1.5).

3.1.1 Pion Multiplicities

The most important point of comparison between theory and experiment is the average number of pions emitted in non-strange annihilations, which we have denoted $\langle n_\pi \rangle$. The lone parameter V in the statistical model must be adjusted to fit the "experimental" value of $\langle n_\pi \rangle$, which is 4.6 ± 0.1 for $\bar{p}p$ (although the result is rather model dependent). In Figure 15 the dependence of $\langle n_\pi \rangle$ on V is shown for various versions of the statistical model. For the old Fermi model, the volume required to match experiment is about $6\Omega_o$, too large to be physically meaningful. For an "intermediate" model including the effects of vector mesons as well as pseudoscalar constituents, we estimate* that once again too large a volume is required. This conclusion differs from that of Barashenkov et al.[31], presumably because they assumed SU(3) symmetry for the masses, while we use the actual experimental values.

For the statistical bootstrap model, which takes into account higher mass resonances and thus favors higher multiplicities, it is found that a volume of $(1.5 \pm 0.4)\Omega_o$, corresponding to a radius $(1.14 \pm 0.10)\lambda\!\!\!^{-}_\pi$, suffices to

---

*The calculation took only crude account of contributions from channels with four or more constituents.

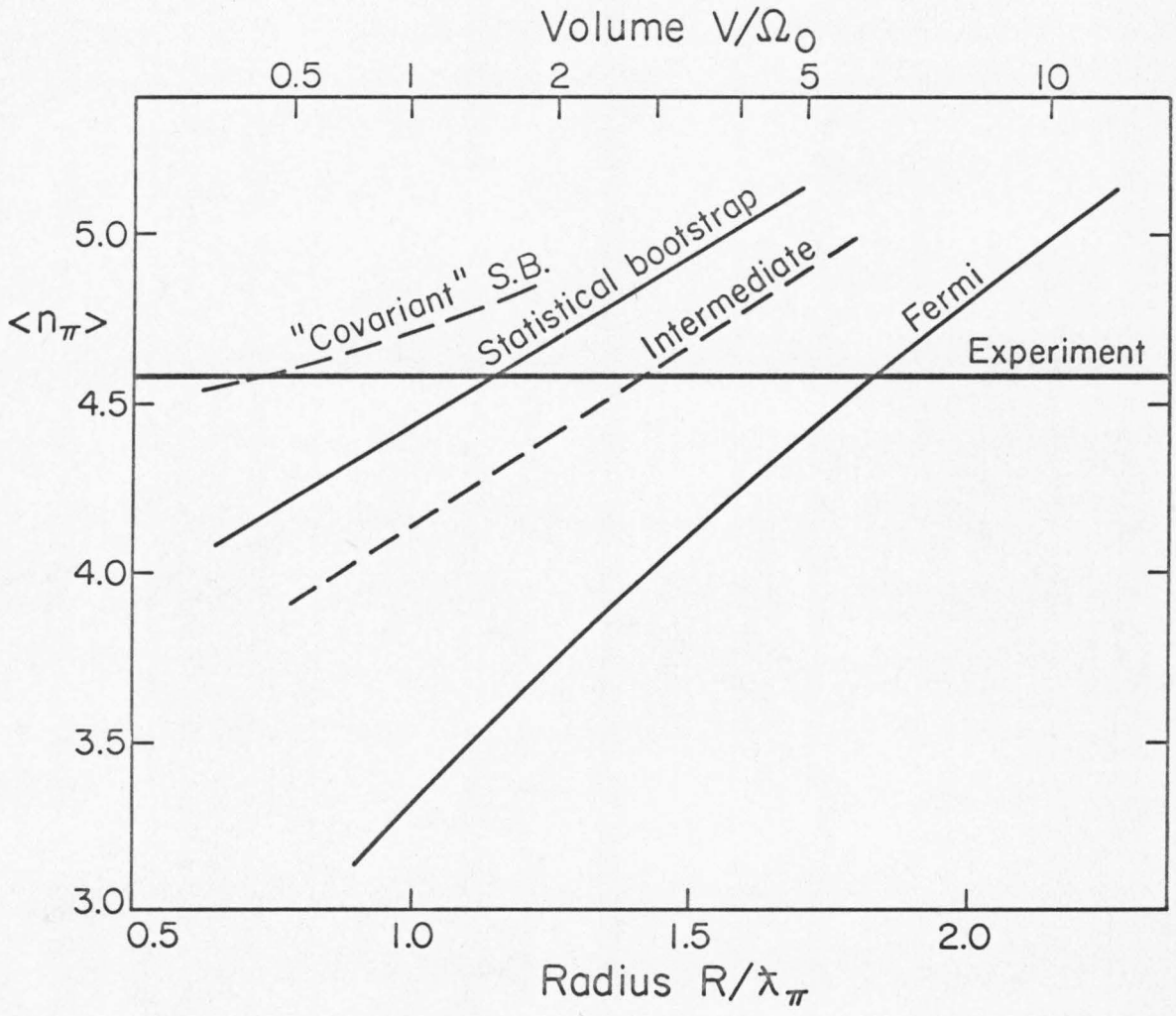

Figure 15. Average pion multiplicity as a function of volume V, for various versions of statistical model.

match $\langle n_\pi \rangle_{expt}$. This is still a little higher than expected, but we feel that it does fall within the bounds of physical plausibility. The corresponding value of T_o is 107 ± 10 MeV, compatible with the value of 120 MeV which we deduce from Hagedorn's results in Section (3.2).

A modification of the model is possible, using the "covariant" phase space expression (Equation [2.1] instead of Equation [1.4]). This type of expression has become popular for its calculational convenience, but there is no theoretical reason to prefer it[57]. The extra factors (m_i/E_i) favor low kinetic energies and thus high final state multiplicities, and so one finds that the volume needed in this version is only $(0.4 \pm 0.3)\Omega_o$, corresponding to a radius $(0.75 \pm 0.18)\lambda\!\!\!^{-}_\pi$ (Figure 15). This would be very satisfactory, but for the fact that the corresponding spectrum of output resonances is much too sparse to be compatible with experiment. For this and other reasons to be discussed below, the original "noncovariant" version is strongly favored. Unless otherwise stated, we shall refer solely to this version in what follows.

3.1.2 Charge Distributions

The branching ratios into specific charge states were deduced from the multiplicity distribution (Figure 6) using

the statistical model for charges* of Pais[58]. The results are compared with experiment in Tables II and III.

The predictions for the average number of charged pions, and the charged prong multiplicity distribution, are accurate to within a couple of percent for $\bar{p}p$ annihilations. For $\bar{p}n$ annihilations, the predicted value for $\langle n_{\pi^\pm} \rangle$ is too low, and the prong distribution reflects this fact. But such a result is to be expected, since the $\bar{p}n$ experimental values were actually obtained in deuterium, where approximately 16% of events involve 3-body interactions[59] which will tend to increase the average pion multiplicity (for instance, $\bar{p}$ annihilations in emulsions gave $\langle n_\pi \rangle \simeq 5.3$, compared with $\langle n_\pi \rangle = 4.6$ for annihilations in hydrogen). So we attach most importance to the $\bar{p}p$ results, and conclude that the prong distributions are reproduced satisfactorily by the model.

When it comes to the branching ratios into specific charge states, however, a few important discrepancies occur.

---

*An alternative procedure would have been to include SU(2) Clebsch-Gordan coefficients in the bootstrap equations (Equation [2.70]), and keep track of charge there. This is a tedious business; and checks indicated that the results would have been quite similar anyway, so the present procedure should be adequate within the accuracy of the calculations.

TABLE II

Relative branching ratios for $\bar{p}p$ annihilation into pions.

Channel	Branching Ratio (%)*	
	Experiment (Ref. 60)	Prediction (R=1.6F)
0 prong	3.4 ± 0.5	1.4
2 prong	44.7 ± 1.2	46.3
$\pi^+\pi^-$	0.34 ± 0.03	0.15
$\pi^+\pi^-\pi^\circ$	8.2 ± 0.9	10.9
$\pi^+\pi^-m\pi^\circ$ (m>1)	36.2 ± 1.3	35.2
4 prong	48.0 ± 1.1	49.1
$2\pi^+2\pi^-$	6.1 ± 0.3	12.7
$2\pi^+2\pi^-\pi^\circ$	19.6 ± 0.9	28.0
$2\pi^+2\pi^-m\pi^\circ$ (m>1)	22.3 ± 1.2	8.4
6 prong	4.0 ± 0.2	3.3
$3\pi^+3\pi^-$	2.0 ± 0.2	2.0
$3\pi^+3\pi^-\pi^\circ$	1.7 ± 0.3	1.1
$3\pi^+3\pi^-m\pi^\circ$ (m>1)	0.3 ± 0.1	0.2
$\langle n_{\pi^\pm} \rangle$	3.05 ± 0.04	3.08

*As a percentage of all events in which no K-mesons are emitted.

TABLE III

Relative branching ratios for $\bar{p}n$ annihilation into pions.

Channel	Branching Ratio (%)*		
	Experiment		Prediction
	Ref. 61	Ref. 65	(R=1.6F)
1 prong	16.4 ± 0.5	17.7 ± 0.7	17.2
$\pi^-\pi^\circ$	$\leq$0.7	0.75 ± .15	0.45
3 prong	59.7 ± 1.2	59.1 ± 0.2	66.8
$2\pi^-\pi^+$	1.57 ± 0.21	2.3 ± 0.3	2.7
$2\pi^-\pi^+\pi^\circ$	21.8 ± 2.2	13.7 ± 2.0	44.5
5 prong	23.4 ± 0.7	22.8 ± 0.9	15.5
$3\pi^-2\pi^+$	5.15 ± 0.47	4.2 ± 0.2	5.4
$3\pi^-2\pi^+\pi^\circ$	15.1 ± 1.0	6.9 ± 0.4	9.0
7 prong	0.39 ± 0.07	0.35 ± .03	0.4
$\langle n_\pi \pm \rangle$	3.15 ± 0.03		2.98

*As a percentage of all events in which no K-mesons are emitted.

For instance, the model predicts that $\bar{p}n \to 2\pi^+\pi^-\pi^\circ$ over 40% of the time, and that this should be the most important single final state: the reason being that $n_\pi=4$ and 5 are much the most common multiplicities (Figure 6), and $n_\pi=4$ is favored over $n_\pi=5$ by a factor 3 to 1 due to the G parity selection rule discussed in the previous Section. These arguments seem hard to evade, and it is therefore disturbing to find that the experimental branching ratio is only 20%, or less. Now in identifying an event as belonging to this channel, various "cutoff" criteria have been applied in the experiment[61], and one might suspect that a significant fraction of events were thus thrown away: but the quoted error seems to exclude this possibility. The discrepancy thus remains a puzzle. Similarly in $\bar{p}p$ annihilation the model predicts that the $2\pi^+2\pi^-$ and $2\pi^+2\pi^-\pi^\circ$ channels should be 50-100% more common than they are found to be experimentally*. For other channels, the model is in reasonable agreement with experiment.

*Recent experimental evidence (C. Ghesquière, Aix-en-Provence conference on elementary particles, Sept. 1970) indicates that these discrepancies are symptomatic of the fact that neutral pions are about 30% more abundant than the statistical model predicts. The reason for this is unknown. Perhaps it is due to the effect of Bose statistics, which we have neglected. This effect would favor low kinetic energies, high multiplicities and symmetric space and charge configurations of the final state pions.

We note at this stage that very similar distributions are obtained in any version of the statistical model, including Fermi's original one, once the average multiplicity is adjusted to the same value. So the successes and failures above are not peculiar to the statistical bootstrap.

3.1.3 Strange Particle Production

Statistical considerations generally predict that K-mesons will be emitted in too large a fraction of the annihilation events[33]. This is true once again in the present model, where $K\bar{K}$ pairs are predicted to occur in 24% of $\bar{p}p$ annihilations and 23% of $\bar{p}n$ annihilations, whereas the experimental figure is around 5 to 7%[28] in both cases.

It seems, therefore, that there must be some dynamical mechanism which suppresses such events. At least part of the answer may lie in Zweig's rule[32], which forbids processes involving disconnected quark diagrams. In the present case, this would forbid the production of ϕ mesons, for instance; whereas the statistical bootstrap predicts that the ϕ meson will be produced, and then decay into a $K\bar{K}$ pair, in 10% of all events (comprising nearly half of all annihilations with strange particles in the final state). Experimental evidence for this suppression has been given by the CERN-CdF collaboration[62]: they find that

$$\frac{R(\bar{p}p \to \omega^{\circ}\pi^{+}\pi^{-})}{R(\bar{p}p \to \phi\pi^{+}\pi^{-})} = 143 \pm 28$$

whereas a statistical model would predict these two rates to have the same order of magnitude.

In spite of this large initial discrepancy between theory and experiment as to the overall rates, it is of interest to make more detailed comparisons for the relative rates in specific $K\bar{K}n\pi$ channels. In Table IV the experimental results for $\bar{p}n$ annihilation[63] are compared with rough values obtained from the model by the procedure mentioned in the last footnote (n=2 only). It can be seen that the model predicts a disproportionately large number of events involving neutral $K\bar{K}$ pairs, in line with the conclusion that $\phi \to K\bar{K}$ events and others like them are suppressed. But the average number of pions emitted with the $K\bar{K}$ pairs, and their multiplicity distribution, are correctly reproduced. Once again these results would occur in other versions of statistical model besides the statistical bootstrap.

3.1.4 Non-strange 2-Body Annihilation Channels

Over the past several years a great deal of information has been accumulated on resonance production in $N\bar{N}$ annihilation at rest. Comparisons with these results can be used to distinguish between various versions of the statistical

TABLE IV

Relative branching ratios for strange $\bar{p}n$ annihilations.

Channel	Branching Ratio (%)[a] Experiment[b]	Prediction (R=1.6F)
$K\bar{K}$	4.4 ± 0.6	2
$K^\circ K^-$	4.4 ± 0.6	2
$K\bar{K}\pi$	25.6 ± 2.1	29
$K^\circ K^-\pi^\circ$	10.6 ± 1.2	6
$K^\circ \bar{K}^\circ \pi^-$	15.0 ± 1.6	23
$K\bar{K}2\pi$	(53)	63
$K^\circ K^-\pi^+\pi^-$	10.1 ± 1.0	7
$K^\circ K^- 2\pi^\circ$	(5)	3
$K^\circ \bar{K}^\circ \pi^-\pi^\circ$	(30)	66
$K^\circ K^+ 2\pi^-$	7.3 ± 0.8	7
$K\bar{K}3\pi$	(17)	5
$K^\circ K^-\pi^+\pi^-\pi^\circ$	9.9 ± 1.1	~0
$K^\circ K^- 3\pi^\circ$	(2)	~0
$K^\circ \bar{K}^\circ \pi^- 2\pi^\circ$	(2)	2
$K^\circ \bar{K}^\circ \pi^+ 2\pi^-$	2.2 ± 0.8	3
$\bar{K}^\circ K^+ 2\pi^-\pi^\circ$	0.5 ± 0.3	~0
$K\bar{K}4\pi$	-	1
$\langle n_\pi \rangle$	(1.83)	1.79

[a] As a percentage of all strange annihilations.

[b] Data extracted from Ref. 63. The figures in brackets are not direct measurements, but have been crudely estimated using statistical assumptions such as $R(K\bar{K}\pi^+\pi^-) = 2 \times R(K\bar{K}2\pi^\circ)$, $R(K^\circ,K^\circ,x^-) = \frac{1}{4} \times R(K^\circ\bar{K}^\circ x^-)$, etc.

model, which up until now have all given rather similar results once the volume V was adjusted to fit $\langle n_\pi \rangle$. The original Fermi version, for instance, took no account of resonance production at all. The "intermediate" version[31] can account for the production of pseudoscalar and vector mesons, but tends to overestimate the branching ratios for channels (especially 2-body channels) involving these particles; it has nothing to say about channels involving other resonances. The statistical bootstrap picture, on the other hand, is an attempt to take all resonances into account in an average, statistical way: the branching ratio into any particular channel can be found by the prescription outlined previously*.

In Table V the model results are compared with experiment for various 2-body channels. Now in making this comparison we are beset by various difficulties:

---

*At this point, it may again be asked how we can justify neglecting the effects of angular momentum conservation. The answer is that angular momentum barrier effects are not important in the particular channels discussed, because the kinetic energy is large. Rough estimates indicate that the inclusion of conservation of angular momentum would alter our branching ratios by amounts of order 30%, a good deal less than the size of the expected statistical fluctuations. It would also tend to reduce the required interaction radius somewhat (F. Cerulus, *Nuovo Cimento 22*, 958 [1961]). Our overall conclusions should not be affected.

TABLE V

Branching ratios for non-strange 2-body annihilations.

Channel	Branching Ratio (%)*			
	Experiment		Theory	
	Ref. 60, 64	CERN-CdF (Ref. 28)	"Noncovariant" R = 1.6F	"Covariant" R = 1.1F
$\bar{p}p$				
$\pi^+\pi^-$	0.33 ± .03		0.15	0.04
$\rho^\circ\pi^\circ$	1.5 ± 0.2	2.0 ± 0.3	0.4	0.9
$\rho^\pm\pi^\mp$	2.8 ± 0.4	4.1 ± 0.3	1.7	3.3
$\omega^\circ\pi^\circ$			0.8	1.6
$B^\pm\pi^\mp$	0.79 ± .26	0.8 ± 0.1	0.9	3.5
$f^\circ\pi^\circ$		0.25 ± .05	0.9	3.6
$A_2^\pm\pi^\mp$		2.1 ± 0.3	1.1	4.4
$\eta^\circ\rho^\circ$	0.23 ± 0.18	0.7 ± 0.2	0.2	1.5
$\rho^\circ\rho^\circ$	0.4 ± 0.3	0.13 ± 0.13	0.4	3.8
$\omega^\circ\rho^\circ$	0.7 ± 0.3	2.4 ± 0.2	2.1	23.0
TOTALS	6.7 ± 0.7	12.5 ± 0.6	5.9 7.9	36.0 44.0

TABLE V (continued)

Channel	Branching Ratio (%)*			
	Experiment		Theory	
	Ref. 61	CERN-CdF Ref. 65	"Noncovariant" R = 1.6F	"Covariant" R = 1.1F
$\bar{p}n$				
$\pi^\circ\pi^-$	<0.7	0.75 ± .15	0.45	
$\rho^\circ\pi^-$	0.63	0.05 ± .05	0.4	
$\omega^\circ\pi^-$	0.41 ± .08	0.33 ± .04	2.4	
$\phi\ \pi^-$		0.07 ± .004	1.2	
$f^\circ\pi^-$	0.94	1.1 ± 0.4	0.7	
$A_2^\circ\pi^-$	<3.3	<0.5	1.8	

*As a percentage of all events in which no K-mesons are emitted.

i) In an experiment, the resonance contribution always has to be separated from a background, which is difficult to do unambiguously. Thus the two groups quoted in Table V which have investigated $\bar{p}p$ annihilation channels sometimes disagree with each other by factors of 3 or more;

ii) A statistical model cannot pretend to predict the coupling of an individual 2-body channel to the $N\bar{N}$ system with any certainty (see Section [3.1.5]). Upon taking the sum over many channels, however, "random" variations in the couplings should average out, and statistical factors should become dominant: otherwise a statistical treatment is worthless.

Because of these facts, it is not surprising to find that the theory fails to predict the individual 2-body branching ratios accurately. The discrepancies show no systematic pattern, though, and when one looks at the totals over all $\bar{p}p$ channels the model has more success. The theoretical totals are actually too low by 10 to 40%, but this is not a very significant amount statistically, since the rates in individual channels are off by factors of up to 4. For the sake of completeness, nevertheless, it is worth noting that a 20% increase in the theoretical totals could be achieved by lowering the radius R by about 0.1 fermi, which is within the allowed limits set in Section (3.1.1).

A similar comparison with the "covariant" version of the statistical bootstrap exposes some severe shortcomings (Table V). This model clearly gives undue importance to channels involving high mass particles, and predicts totals over all the measured two-body channels which are far too high. [This complements the previous statement (Section (3.1.1)) that the resonance spectrum was too sparsely populated at high masses in this version: the small numbers in the high-mass spectrum are compensated by their undue relative weight in the branching ratios, leading to the same final pion multiplicities as in the "noncovariant" version.]

3.1.5 Statistical Fluctuations

These fluctuations are an intrinsic part of the theory, and some understanding of them is necessary in order to judge our results. The problem may again be treated using the methods of the statistical theory of compound nuclear reactions. The rate at which an $N\bar{N}$ pair annihilates into a given final state f can be written:

$$R(N\bar{N} \to f) \propto \sum_c \sum_{j_c=1}^{n_c} |\gamma_{N\bar{N},j_c}|^2 \, |\gamma_{j_c,f}|^2 \qquad (3.3)$$

where $\sum_c$ denotes the sum over all channels c contributing to the final state f and $\sum_{j_c}$ denotes the sum over all resonances

j_c contributing to the channel c at that energy (i.e. within an energy interval of order the width of a resonance, which we shall take to be about m_π). The γ's are coupling constants which are assumed to vary randomly.

But since the intermediate resonances j are taken to form a complete set of states in this problem, then corresponding to any partition of the $N\bar{N}$ annihilation products into states f (for example, i) first generation decay products, or ii) ultimate final states consisting of "stable" particles) we can choose a set of basis states $\{j_{cf}\}$ such that $j_{cf} \to f$ <u>only</u>, and

$$R(N\bar{N} \to f) \propto \sum_c \sum_{j_{cf}=1}^{n_{cf}} |\gamma_{N\bar{N},j_{cf}}|^2 \Gamma^{tot}_{j_{cf}} \qquad (3.4)$$

For heavy resonances, where the number of decay channels is large, the total widths should become <u>uniform</u>[4]. Then the expected relative fluctuations in $R(N\bar{N} \to f)$ are proportional to $(\sum_c n_{cf})^{-\frac{1}{2}}$, while one expects $R(N\bar{N} \to f) \propto (\sum_c n_{cf})$ itself. Therefore, the expected relative fluctuations decrease as one on the square root of $R(N\bar{N} \to f)$.

This argument ignores interference terms between resonances, variations in SU(3) couplings, and so on, as is usually done in the Bohr model.

Now the spectrum generated in the numerical analysis, when one takes account of the various quantum number conservation laws (including J and G), contains of order 60

different resonances which should couple to the $N\bar{N}$ system at rest (i.e., within $\Delta E = m_\pi$ of that energy). The predicted branching ratios $N\bar{N} \rightarrow$ (2-body final state) are all of order 0.01; so each 2-body final state couples to 0.6 resonances, on the average. Therefore, the expected fluctuations in these branching ratios should be of a similar order of magnitude to the fluctuations in the single channel partial widths $\Gamma_{N^* \rightarrow N_\pi}$, as one goes from resonance to resonance in the Particle Data Group tables[15]. This checks out quite well: in both cases the fluctuations are of order 100%, corresponding to factors of order 2.

From this starting point, the expected fluctuations in the branching ratios for the various ultimate reaction products can now be estimated. For instance, the predicted branching ratio into $K\bar{K}n\pi$ final states is about 0.25, so the expected percentage fluctuation away from this figure is only 1/5 of the 2-body fluctuations, i.e., around 20%. In fact, the experimental branching ratio is only about 0.07, too small by a factor of 4. This is clearly outside the expected error limits, and indicates the presence of some systematic or dynamical effect of the type already discussed in Section (3.1.3).

The predicted branching ratios for $\bar{p}p \rightarrow$ 2-prong and 4-prong (non-strange) final states approach 0.5 each: so the expected error in these branching ratios would be about 15%, on the basis of the above ideas. In fact, these

branching ratios are predicted to within an accuracy of less than 4%. The reason for the greater accuracy is presumably the fact that we have adjusted the volume V to fit $\langle n_\pi \rangle$. If we had been given the "correct" value of V a priori, the above arguments suggest that the predicted value of $\langle n_\pi \rangle$ could have been in error by about 4%. Turning this reasoning around, it follows that the experimental multiplicity $\langle n_\pi \rangle \simeq 4.6$ may correspond to quite a large range of values of the radius R, namely $R = (1.14 \pm 0.18)\lambda\!\!\!^{-}_\pi$, if one allows for statistical fluctuations.

3.1.6 Conclusions

We conclude that the model is generally successful as a phenomenological description of $N\bar{N}$ annihilation at rest, except that some account needs to be taken of the dynamical effect which suppresses strange particle production.

In all the aspects of Sections (3.1.1) through (3.1.3), the original Fermi model and its subsequent modifications gave very similar results to those of the statistical bootstrap, except that implausibly large values of the "interaction radius" were required to fit experiment. It is only when one looks at resonance production (Section [3.1.4]) that one is able to distinguish between the various models on phenomenological grounds. Here the advantage of the statistical bootstrap is clearly evident, in that it

endeavors to include the effects of all the resonances in the spectrum, and treats them all on an equal footing. From this point of view, previous models have been definitely incomplete.

A brief discussion of statistical fluctuations was given. These determine the expected error associated with the statistical predictions, and form an intrinsic part of the theory. Rough estimates of their magnitude were used as a basis for judgement in the experimental comparisons above.

Because of these statistical fluctuations, our fit to the $N\bar{N}$ annihilation results is not expected to be an accurate way of determining the volume V. The box radius required to fit the experimental pion multiplicity was 1.6 fermi, but there is a likely error of ±0.25 fermi associated with the result. Nevertheless, this radius is much more plausible physically than the value R = 2.6 fermi required in the old Fermi model.

3.2 General Features of Resonance Decay

The features of resonance decay predicted by the statistical bootstrap were summarized in Section (1.2.2) of the Introduction. Here we shall discuss the momentum distribution of the emitted pions in more detail.

A large proportion of the first generation decays result in a state consisting of one pion plus a heavy resonance. The contribution of such states to the total phase space at mass m (in units $\hbar=c=m_\pi=1$) is proportional to

$$\int_1^{m-1} dm_2 \; \rho_{in}(m_2) \int_0^\infty p^2 \, dp \; \delta(\sqrt{1+p^2} + m_2 - m) \tag{3.5}$$

$$\underset{m\to\infty}{\sim} cm^{-3} \; e^{\beta_0 m} \int_0^\infty p^2 \, dp \; e^{-\beta_0\sqrt{1+p^2}} \;, \; p<<m \tag{3.6}$$

The probability of finding one of these pions with momentum p is therefore given by

$$P(p) \underset{m\to\infty}{\propto} p^2 \exp\left[-\beta_0\sqrt{1+p^2}\right] \tag{3.7}$$

Hence the average kinetic energy per pion can be calculated in terms of modified Bessel functions

$$\langle T_\pi \rangle = \frac{3K_3(\beta_0) + K_1(\beta_0)}{4K_2(\beta_0)} - 1 \tag{3.8}$$

In the non-relativistic limit, this reduces to

$$\langle T_\pi \rangle \underset{\beta_0\to\infty}{\sim} {}^3/_2 \; \beta^{-1} = {}^3/_2 \; T_0 \tag{3.9}$$

which is just the ½ T_0 per degree of freedom one would expect in classical thermodynamics.

Now the average number of pions emitted by the resonance is related to $\langle T_\pi \rangle$:

$$\langle n_\pi \rangle \underset{m\to\infty}{\sim} \frac{m}{m_\pi + \langle T_\pi \rangle} \tag{3.10}$$

But the slope of the line $\langle n_\pi \rangle$ versus m shown in Figure 5 is about 25% less than one would have estimated from Equations (3.8) and (3.10). There are several factors which might contribute to this effect:

i) Most important is the emission of other light particles besides the π (such as η, ρ, ω, etc.), which may occur at any stage along the decay chain. These particles will carry away appreciable kinetic energies (again, of order 3/2 T_o) before disintegrating into pions, and thus will tend to increase the average kinetic energy $\langle T_\pi \rangle$.

ii) The decay modes of the low-mass input states have been put in by hand, and may deviate from the thermodynamic or statistical predictions. But a glance at Figure 5 shows that this deviation is not large.

iii) The kinetic energy of the heavy secondary resonances relative to the original center of mass will tend to increase from one generation to the next; but this is only important towards the end of the chain, and will have a negligible effect on $\langle T_\pi \rangle$ when the initial mass is large.

iv) The internal temperature of a finite-mass resonance actually tends to be higher than T_o, as was recently shown by Carlitz[42]. Again, this effect dies away as the initial mass gets large.

This discrepancy in slope will have important practical consequences. It means that the "effective temperature" obtained by fitting a Planck-type distribution

$$P(p_\pi) \propto p_\pi^2 \exp[-E_\pi/T_{eff}] \qquad (3.11)$$

to the experimental high-energy momentum spectra will be about 25% larger than T_o. In particular, Hagedorn's results for high-energy transverse momentum distributions[9] show $T_{eff} \simeq 160$ MeV: this would correspond to $T_o \simeq 120$ MeV, and a box radius R very close to $\lambda\!\!\!^{-}_\pi$. Such a value of T_o agrees reasonably well with the value 107 ± 20 MeV which we obtained in fitting $N\bar{N}$ annihilation at rest.

Hagedorn himself has noted[9] that decays in second and later generations would tend to raise T_{eff} above T_o, i.e. to broaden the momentum spectrum of emitted particles. But up until now he has used a mass spectrum $\rho(m) \sim cm^a e^{\beta_o m}$ with $a = -5/2$ (rather than -3), which implies a logarithmic increase in the multiplicity of first generation decay products as a function of the mass of the decaying resonance. This makes it very difficult to perform phase space calculations, and to compute effects beyond the first generation.

He was thus unable to make any quantitative estimate of the difference between T_{eff} and T_o. In the present "strong bootstrap" version, on the other hand, one can neglect states with more than three constituents emerging from each vertex, and the phase space calculations are much more simple.

Finally, it must be observed that the momentum distribution (3.11) is only an approximation, even with T_o replaced by T_{eff}. At small momenta the Bose statistics make themselves felt, and the distribution will look more like:

$$P(p_\pi) \propto p_\pi^2 \frac{1}{e^{E_\pi/T_{eff}} - 1} \tag{3.12}$$

A nice experimental demonstration of this effect was recently given by Erwin et al.[66] At large momenta, on the other hand, the approximation $m_2 \simeq m$ made in Equation (3.6) begins to break down. Then one has:

$$P(p_\pi) \propto p_\pi^2 \, m_2^{-3} \, e^{\beta_o m_2} = p_\pi^2 (m^2 - 2mE_\pi + 1)^{-3/2}$$

$$\exp\{\beta_o [m^2 - 2mE_\pi + 1]^{\frac{1}{2}}\} \tag{3.13}$$

where $\beta_o \to \beta_{eff}$ when second and later generations are added in. This behavior has been checked in a computer model and confirmed to occur. Phenomenologically, it will result in a steepening of the exponential fall-off at large momenta.

It is a feature which may be important at large transverse momenta in high-energy collisions[6 7].

IV. CONCLUSIONS

An overall review of the present status of the statistical bootstrap model was given in Chapter I. In order to minimize any "double counting" of the conclusions, we shall restrict ourselves at this point to a recapitulation of those results contributed by the present author, working largely in collaboration with Frautschi[12,29].

In connection with the level density, the first treatment of the distribution of levels as a function of internal quantum numbers was given by Hamer and Frautschi[12] - see Section (2.3). This enabled them to construct a realistic hadron spectrum (Section [2.4]): its asymptotic form was later derived analytically by Nahm[13]. From this work, it was possible to conclude:

1) The analytical results of Nahm[13] were generally in good agreement with the numerical results of Hamer and Frautschi[12]. This provides a check of the uniqueness and convergence of the analytical solution (Section [2.1]).

2) Alternative methods of choosing a low-mass input spectrum give very similar results (Section [2.4]), so it is possible in practice to find an essentially unique "realistic" bootstrap spectrum once a value for the radius R is specified.*

*And assuming the absence of "exotic" states.

3) For values of R near $\lambda\!\!\!^{-}_{\pi}$, the resulting spectrum bears a reasonable resemblance to experiment at energies where the experimental spectrum is well known ($\lesssim$ 1.5 GeV). This comparison provides no real evidence in favor of the model, but proves that it is at least compatible with experiment.

In the present work, the treatment of quantum numbers has been redone, using the powerful Laplace transform technique of Nahm[13]. In the case of an unrestricted additive number Q, this has enabled us to find an equation for d, the parameter involved in the Gaussian distribution function $\exp(-dQ^2/m)$ - see Section (2.3). The treatment of angular momentum due to Chiu and Heimann[11] has been modified in the same way, showing that the Gaussian form for the spin distribution is indeed unique.

A statistical model for hadronic reactions has been developed[29,35], analogous to the Bohr model in nuclear physics, which makes use of the hadron level density. It was applied to the case of $N\bar{N}$ annihilation at rest[29] (Section 3.1), where it turned out that the high multiplicity of final state pions, together with the low branching ratios into specific 2-body final states involving resonances, could be explained using a radius R = 1.6 ± 0.25 fermi. The results also indicated the presence of a systematic dynamical effect suppressing strange particle production.

It could thus be concluded that by giving the radius R a value of approximately $\lambda\!\!\!^{-}_{\pi}$, which is quite reasonable physically, one can simultaneously obtain:

1) A bootstrap spectrum reasonably compatible with experiment;

2) An explanation of the major features of $N\bar{N}$ annihilation at rest (barring the suppression of strange particle production);

3) A fit to high-energy transverse momentum distributions à la Hagedorn[9] (since the corresponding value of T_{eff} is about 160 MeV - Section [3.2]);

4) A successful description of the "Ericson fluctuations" in hadron physics discussed by Frautschi[35].

Thus the model gives quantitatively* consistent results in several different areas of hadron physics.

Finally, the model was used to deduce some general features of resonance decay[29] (for "resonance", one may also read "cluster", "fireball", "nova" or any other object whose decay is governed by statistical factors). This decay chain was investigated in detail (Sections [1.2.2] and [3.2]), and a linear rise in the average final state multiplicity with the initial mass was demonstrated. It was shown that the multiplicity distribution is roughly Gaussian. The momentum distribution of the reaction

*To order 10% or so.

products was studied, and the effects of secondary decays on the distribution were shown to result in a 25% increase in the "effective temperature". A form valid towards the high-momentum tail of the distribution was given[6 7] (Equation [3.13]). It is unlikely that these features can be tested directly by experiment, because of the difficulty of isolating high mass resonances. But they may be tested indirectly via some model of high-energy reactions.

REFERENCES

1. L. D. Landau and E. M. Lifshitz, "Statistical Physics" (Addison-Wesley, 1958), Ch. 1.

2. N. Bohr, Nature 137, 344 (1936); N. Bohr and F. Kalckar, K. Danske Vidensk. Selsk. mat.-fys. Medd. 14, 10 (1937). For an up-to-date review, see E. Vogt, Advances in Nuclear Physics 1, 261 (1968).

3. H. A. Bethe, Phys. Rev. 50, 332 (1936); Rev. Mod. Phys. 9, 69 (1937). A modern review is T. Ericson, Advances in Physics 9, 425 (1960).

4. M. A. Preston, op. cit.

5. V. F. Weisskopf, Phys. Rev. 52, 295 (1937).

6. J. D. Jackson, Canad. J. Phys. 34, 767 (1956); K. J. Le Couteur, Proc. Phys. Soc. A65, 718 (1952); and for a recent experimental comparison, see K. Tsukuda, S. Tanaka, M. Maruyama and Y. Tomita, Nucl. Phys. 78, 369 (1966).

7. C. F. Porter and R. G. Thomas, Phys. Rev. 104, 483 (1956).

8. M. L. Mehta and M. Gaudin, Nucl. Phys. 18, 420 (1960).

9. R. Hagedorn, Nuovo Cimento Suppl. 3, 147 (1965).

10. S. Frautschi, Phys. Rev. D3, 2821 (1971).

11. C. B. Chiu and R. L. Heimann, Phys. Rev. D4, 3177 (1971).

12. C. J. Hamer and S. C. Frautschi, Phys. Rev. D4, 2125 (1971).

13. W. Nahm, preprint PI2-102 (Bonn).

14. R. Hagedorn, Suppl. Nuovo Cimento 6, 311 (1968).

15. N. Barash-Schmidt et al., Phys. Letters 33B, No. 1 (1970).

16. S. Fubini and G. Veneziano, Nuovo Cimento 64A, 811 (1969); K. Bardakci and S. Mandelstam, Phys. Rev. 184, 1640 (1969); S. Fubini, D. Gordan and G. Veneziano, Phys. Letters 29B, 679 (1969); P. Oleson, Nucl. Phys. B18, 459 (1970) and B19, 589 (1970).

17. A. Krzywicki, Phys. Rev. 187, 1964 (1969); R. Brout (unpublished).

18. K. Huang and S. Weinberg, Phys. Rev. Letters 25, 895 (1970).

19. E. Beth and G. E. Uhlenbeck, Physica 4, 915 (1937). For recent treatments, see L. Landau and E. Lifshitz, "Statistical Physics", 2nd ed., Sec. 77 (Pergamon Press 1969); R. Dashen, S. Ma and H. J. Bernstein, Phys. Rev. 187, 345 (1969).

20. S. Z. Belenky, Nucl. Phys. 2, 259 (1956).

21. This argument was given by R. Hagedorn, Ref. 34.

22. E. Wigner, Phys. Rev. 98, 145 (1955).

23. S. Mandelstam, Phys. Rev. 166, 1539 (1968); Comments on Nuclear & Particle Physics 3, 3, 65 (1969).

24. L. van Hove, Phys. Letters 24B, 183 (1967).

25. L. Durand III, Phys. Rev. 161, 1610 (1967).

26. E. Fermi, Prog. Theor. Phys. 5, 570 (1950).

27. For a review of early work see M. Kretzschmar, Ann. Revs. Of Nuclear Science 11, 1 (1961).

28. For experimental reviews see R. Armenteros and B. French, "High Energy Physics" (ed. E. Burhop, Academic Press, 1969), Vol IV, p. 237; L. Montanet, Proc. Lund Int. Conf. on E. P.'s, p. 189 (1969); N. Gelfand, and T. E. Kalogeropoulos, in "Symposium on $N\bar{N}$ Interactions" (Argonne, 1968).

29. C. J. Hamer, Caltech preprint CALT 68-346 (submitted to Nuovo Cimento).

30. F. Cerulus, Nuovo Cimento 14, 827 (1959).

31. V. S. Barashenkov, V. M. Maltsev and G. M. Zinoviev, Acta Physica Polonica 33, 315 (1968).

32. G. Zweig, CERN Reports TH 401 and TH 412 (1964), unpublished.

33. See e.g. Ref. 27 or S. C. Frautschi, Prog. Theor. Phys. 22, 15 (1959).

34. R. Hagedorn, unpublished lectures CERN 71-12 (1971).

35. S. Frautschi, CERN Preprint TH 1463 (1972).

36. T. Ericson, Phys. Rev. Letters 5, 430 (1960), and Ann. Phys. (N.Y.) 23, 390 (1963); T. E. O. Ericson and T. Mayer-Kuckuk, Ann. Rev. Nucl. Sci. 16, 183 (1966).

37. Allaby et al., Phys. Letters 23, 389 (1966); Akerlof et al., Phys. Rev. 159, 1138 (1967); Brabson et al., Phys. Rev. Letters 23, 1306 (1969).

38. C. Michael, Phys. Letters 29B, 230 (1969).

39. R. Hagedorn and J. Ranft, Suppl. Nuovo Cimento 6, 169 (1968); and further references to be found in Ref. 34.

40. J. Orear, Phys. Letters 13, 190 (1964).

41. Yu. M. Antipov et al., Sov. J. Nucl. Phys. 12, 171 (1971) [translation of Yad. Fiz. 12, 311 (1970)]; and other references quoted by Hagedorn in Ref. 14.

42. See for instance S. J. Chang and R. Rajaraman, Phys. Rev. 183, 1517 (1969); V. N. Akimov, D. S. Chernavskii, I. M. Dremin and I. I. Royzen, Nucl. Phys. B14, 285 (1969); I. G. Halliday, Nucl. Phys. B21, 445 (1970); A. Bassetto and F. Paccanoni, Nuovo Cimento 2A, 306 (1971).

44. G. Ranft and J. Ranft, Phys. Letters 32B, 207 (1970).

45. For a recent review of multiperipheralism and many-particle production, see D. Horn, CERN preprint TH 1387 (to be published in "Physics Reports").

46. P. G. O. Freund, Phys. Rev. Letters 20, 235 (1968); H. Harari, Phys. Rev. Letters 20, 1395 (1968).

47. K. Igi and S. Matsuda, Phys. Rev. Letters 18, 625 (1967); R. Dolen, D. Horn and C. Schmid, Phys. Rev. 166, 1768 (1968).

48. Ya. B. Zeldovich, Comments Astrophys. Space Phys. 2, 12 (1970).

49. This quotation is from S. Frautschi, Ref. 10. For further discussions, see S. Frautschi, G. Steigman and J. Bahcall (submitted to the Astrophysical Journal), and references therein.

50. S. Frautschi, J. N. Bahcall, G. Steigman and J. C. Wheeler, Comments Astrophys. Space Phys. 3, 121 (1971).

51. P. P. Srivastava and G. Sudarshan, Phys. Rev. 110, 765 (1958).

52. F. Cerulus, Nuovo Cimento 22, 958 (1961).

53. C. B. Chiu, R. L. Heimann and A. Schwimmer, Phys. Rev. D4, 3184 (1971).

54. J. J. de Swart, Rev. Mod. Phys. 35, 916 (1963).

55. B. R. Desai, Phys. Rev. 119, 1385 and 1390 (1960).

56. R. Armenteros et al., Proc. Int. Conf. High Energy Phys., CERN 1962 (ed. J. Prentki), p. 351.

57. R. Hagedorn, "Relativistic Kinematics" (Benjamin, 1963), p. 89.

58. A. Pais, Ann. Phys. (N. Y.) 9, 548 (1960); see also F. Cerulus, Suppl. Nuovo Cimento 15, 402 (1960).

59. R. Bizzarri et al., Lettere al Nuovo Cimento 2, 431 (1969); Ciapetti et al., Suppl. Nuovo Cimento 3, 1208 (1965).

60. C. Baltay, P. Franzini, G. Lütjens, J. C. Severiens, D. Tycko and D. Zanello, Phys. Rev. 145, 1103 (1966).

61. A. Bettini, M. Cresti, S. Limentani, L. Peruzzo, R. Santangelo, S. Sartori, L. Bertanza, A. Bigi, R. Carrara, R. Casali and P. Lariccia, Nuovo Cimento 47, 642 (1967).

62. R. Bizzarri, M. Foster, Ph. Gavillet, G. Labrosse, L. Montanet, R. Salmeron, P. Villemoes, C. Ghesquière and E. Lillestøl, Nucl. Phys. B14, 169 (1969).

63. A. Bettini, M. Cresti, S. Limentani, L. Peruzzo, R. Santangelo, S. Sartori, L. Bertanza, A. Bigi, R. Carrara, R. Casali, P. Lariccia and C. Petri, Nuovo Cimento 62A, 1038 (1969). We have not presented similar results for pp annihilation, because the data there are plentiful but not complete: measurements of channels involving K^+K^- pairs, in particular, are lacking.

64. C. Baltay, J. C. Severiens, N. Yeh and D. Zanello, Phys. Rev. Letters 18, 93 (1967).

65. T. E. Kalogeropoulos, Symposium on $N\bar{N}$ Interactions (Argonne, 1968), p. 17; and private communication of results due to P. Hagerty and L. Gray.

66. J. Erwin, W. Ko, R. L. Lander, D. E. Pellett, and P. M. Yager, Phys. Rev. Letters 27, 1534 (1971).

67. S. Frautschi and C. Hamer, forthcoming publication.